IGOR MARTINS GONÇALVES

PRETREATMENT OF BAGASSE, STRAW, AND ENERGY SUGARCANE USING NIOBIUM PHOSPHATE CATALYST

Dissertation submitted to the Agrochemistry Graduate Program of the Universidade Federal de Viçosa in partial fulfillment of the requirements for the degree of *Magister Scientiae*..

Adviser: Reinaldo Francisco Teófilo

VIÇOSA - MINAS GERAIS
2023

Ficha catalográfica elaborada pela Biblioteca Central da Universidade Federal de Viçosa - Campus Viçosa

T
G635p
2023

Gonçalves, Igor Marins, 1996-
Pretreatment of bagasse, straw, and energy sugarcane using niobium phosphate catalyst / Igor Marins Gonçalves. – Viçosa, MG, 2023.
1 dissertação eletrônica (62 f.): il. (algumas color.).

Texto em inglês.
Orientador: Reinaldo Francisco Teófilo.
Dissertação (mestrado) - Universidade Federal de Viçosa, Departamento de Química, 2023.
Referências bibliográficas: f. 57-62.
DOI: https://doi.org/10.47328/ufvbbt.2023.267
Modo de acesso: World Wide Web.

1. Nióbio. 2. Catalisadores. 3. Bagaço de cana. 4. Biomassa vegetal. 5. Cana-de-açúcar. 6. Furaldeído. 7. Xilose. 8. Projeto experimental. I. Teófilo, Reinaldo Francisco, 1978-.
II. Universidade Federal de Viçosa. Departamento de Química. Programa de Pós-Graduação em Agroquímica. III. Título.

CDD 22. ed. 546.524

Bibliotecário(a) responsável: Bruna Silva CRB-6/2552

IGOR MARTINS GONÇALVES

PRETREATMENT OF BAGASSE, STRAW, AND ENERGY SUGARCANE USING NIOBIUM PHOSPHATE CATALYST

Dissertation submitted to the Agrochemistry Graduate Program of the Universidade Federal de Viçosa in partial fulfillment of the requirements for the degree of *Magister Scientiae*.

APPROVED: February 28, 2023.

Assent:

Igor Martins Gonçalves
Author

Reinaldo Francisco Teófilo
Adviser

ACKNOWLEDGEMENTS

Primeiramente gostaria de agradecer à minha família, meu pai Gilson, minha mãe Maria Goretti e meu irmão Hugo pelo suporte durante todo este período.

À Universidade Federal de Viçosa, e ao meu orientador Professor Reinaldo pela oportunidade e confiança em mim depositada.

Aos meus amigos que conheci durante a graduação, Gabriel, Jamille, Samira, Alexsandra, Jéssica e Diana. Aos amigos que vieram comigo para universidade, Lucas, Vilela, Heitor e Rafael. Todos estes me proporcionaram bons momentos em Viçosa.

A todos do MCDA Lab. Ao Diego pela parceria em diversos trabalhos durante o mestrado. Ao Helder e Wilson pelos conselhos. À Jussara pelos conhecimentos passados no período que esteve aqui. Aos estagiários, Victória, Ana Barbara, Tales, Ana Julia e Raiane pela contribuição na parte experimental do trabalho. Em especial à Victória, que no período de um ano como estagiária participou em grande parte dos experimentos desta dissertação.

A todos os outros que colaboraram diretamente ou indiretamente para este trabalho

O presente trabalho foi realizado com apoio da Coordenação de Aperfeiçoamento de Pessoal de Nível Superior – Brasil (CAPES) – Código de Financiamento 001.

À Coordenação de Aperfeiçoamento de Pessoal de Nível Superior (CAPES), pela concessão da bolsa de estudos.

ABSTRACT

GONÇALVES, Igor, M.Sc., Universidade Federal de Viçosa, February, 2023. **Pretreatment of bagasse, straw, and energy sugarcane using niobium phosphate catalyst**. Adviser: Reinaldo Francisco Teófilo.

The optimization of hydrothermal pretreatment (HTP) of sugarcane bagasse (SCB), sugarcane straw (SCS), and energy cane (E.C.) using niobium phosphate (NbP) catalyst is the aim of this work. The biomasses were characterized by chemical composition, moisture, and granulometry. The experiments were designed following a face-centered composite design (FCCD), using, as independent variables, temperature (140-180 °C), NbP catalyst load (1-100 %), and time. During HTP, aliquots were taken each 15 minutes and analyzed until they reached 135 minutes. After HTP, the amounts of xylose, arabinose, and furfural (HMF) were determined in the liquor using high-performance liquid chromatography (HPLC). The use of NbP as a catalyst proved to be very effective in the hemicellulose solubilization and the pentoses conversion in furfural. The maximum xylose productivity and best level for temperature and catalyst load were for SCB, SCS, and E.C., respectively 115 g/kg (180 °C and 1%), 71 g/kg (160 °C and 50.5 %), and 61 g/kg (180 °C and 1%). The results showed that furfural production is favored in a high temperature and catalyst load. The maximum furfural productivity predicted by the models were 95 g/kg, 75 g/kg, and 65 g/kg for SCB, SCS, and E.C., respectively.

Keywords: Design of experiments. Bagasse. Catalyst. Energy cane. Sugarcane biomass. Xylose. Furfural.

RESUMO

GONÇALVES, Igor, M.Sc., Universidade Federal de Viçosa, fevereiro de 2023. **Pré-tratamento de cana energia, bagaço e palha de cana de açúcar utilizando fosfato de nióbio como catalisador**. Orientador: Reinaldo Francisco Teófilo.

A otimização do pré-tratamento hidrotérmico (HTP) do bagaço da cana-de-açúcar (SCB), da palha da cana-de-açúcar (SCS) e da cana-energia (EC) utilizando catalisador de fosfato de nióbio (NbP) é o objetivo deste trabalho. As biomassas foram caracterizadas quanto à composição química, umidade e granulometria. Os experimentos foram planejados seguindo um projeto composto de face centrada (FCCD), usando, como variáveis independentes, temperatura (140-180 °C), carga de catalisador NbP (1-100%) e tempo. Durante o HTP, alíquotas foram retiradas a cada 15 minutos e analisadas até atingir 135 minutos. Após HTP, as quantidades de glicose, xilose, arabinose, furfural foram determinadas no licor usando cromatografia líquida de alta eficiência (HPLC). A utilização de NbP como catalisador mostrou-se bastante eficaz na solubilização de hemiceluloses e na conversão de pentoses em furfural. O rendimento máximo de xilose e o melhor nível de temperatura e carga de catalisador foram para SCB, SCS e EC, respectivamente 115 g/kg (180 °C e 1%), 71 g/kg (160 °C e 50,5%) e 61 g /kg (180 °C e 1%). Os resultados mostraram que a produção de furfural é favorecida em alta temperatura e alta carga de catalisador. Os rendimentos máximos de furfural previstos pelos modelos foram 95 g/kg, 75 g/kg e 65 g/kg para SCB, SCS e EC, respectivamente.

Palavras-chave: Planejamento de experimento. Bagaço. Catalisador. Cana-energia. Biomassa da Cana-de-açúcar. Xilose. Furfural.

LIST OF ILLUSTRATIONS

Figure 1. World energy consumption by source over the years 1850 to 2021 (Data source: (OUR WORLD IN DATA, 2021)). 14

Figure 2. Generations of biofuels according to source and process.(PAPAKONSTANTINOU et al., 2021) 16

Figure 3. The general structure of lignocellulosic biomass and its components.(SOLTANIAN et al., 2020) 17

Figure 4 . Sugarcane production worldwide map (a) and leading countries in sugarcane production with respective yield, area, and production (bubble size) (b). (Data source: (FAO, 2021)) 19

Figure 5 . Brazil map of sugarcane production for each state (A) and Brazil map of sugar and ethanol plant for each state (B). (Data source: (COMPANHIA NACIONAL DE ABASTECIMENTO, 2022) (a), NovaCana(NOVACANA, 2022) (b)). 20

Figure 6. Depiction of sugarcane plant and its fractions(NEGRÃO et al., 2021). 21

Figure 7. Representation of the development of sugarcane and energy cane (DE ABREU et al., 2020). 23

Figure 8. Classification of different types of pretreatment methods for lignocellulosic biomass (SOLTANIAN et al., 2020). 24

Figure 9. Schematic structure of $NbOPO_4$. 29

Figure 10. Conversion of xylose (a) and glucose (b) with both Lewis and Bronsted acids. The thicker arrow shows the preferential reaction. The green and blue arrows represent the reactions catalyzed by Lewis and Bronsted acid, respectively.(VIEIRA et al., 2021). 30

Figure 11. Conversion of xylose to furfural by Lewis acid sites (A) and Bronsted acid sites (B).(BHAUMIK; DHEPE, 2016) 31

Figure 12. Fuel components and chemicals derived from furfural(LI; JIA; WANG, 2016). .. 32

Figure 13. Granulometry distribution of SBS 38

Figure 14. The moisture content of sugarcane bagasse (SCB), sugarcane straw (SCS), and energy cane (EC). 39

Figure 15. SCB pretreatment comparison between the absence (A) and the presence (B) of NbP as the catalyst. Experimental conditions: Temperature of 170°C, and for the presence of the catalyst (NbP) was choose a 100 % load. 41

Figure 16. Pretreatments of SCB according to the FCCD. In the horizontal orientation, it shows pretreatments at the same temperature, and in the vertical orientation the same catalyst load. 42

Figure 17. Pretreatments of SCS according to the FCCD. In the horizontal orientation, it shows pretreatments at the same temperature, and in the vertical orientation the same catalyst load.43

Figure 18 Pretreatments of EC according to the FCCD. In the horizontal orientation, it shows pretreatments at the same temperature, and in the vertical orientation the same catalyst load.43

Figure 19. Images of SCB (A to I), SCS (J to R), and EC (S to A1) cellulign after the pretreatment following the respective conditions.....45

Figure 20. Responses surfaces of FF yield as the function of temperature and time and the function of temperature and the catalyst load for SCB (A and B), SCS (C and D), and EC (E and F).....51

Figure 21. x-ray diffractogram of raw cellulose (front), raw sugarcane (middle), and pretreat SCB at 180 °C with 1 % catalyst load (back).....52

Figure 22. x-ray diffractions from different pretreatment conditions for SCB. The experimental conditions were 1% of NbP and temperatures of 140 °C (back), 160 °C (middle), and 180 °C (front).....53

Figure 23. SEM images of SCB before (a and b) and after pretreatment (c and d). Pretreatment conditions: 170 °C and 50 % catalyst load.....54

Figure 24. EDS images of SCB, the original image (A), and the chemical map of carbon (B), oxygen (C), silicon (D), phosphate (E), and niobium (F).....55

LIST OF TABLES

Table 1. Compares sugarcane and energy cane (GRASSI; PEREIRA, 2019).....22

Table 2. Advantages and disadvantages of physical pretreatments. (Soltanian et al., 2020). .25

Table 3. The different processes of furfural production (MARIANA NEVES CATRINCK, 2018).....32

Table 4. FCCD levels and variables 34

Table 5. FCCD with the three independent variables.....35

Table 6. Ashes content for all SBS.....40

Table 7. Chemical composition of raw SBS.....40

Table 8. Independent variables used in FCCD and respective responses of pentoses and FF for SBS.....47

Table 9. Coefficients and lack of fit using pentoses and FF response for SCB.....49

Table 10. Coefficients and lack of fit using pentoses and FF response for SCS.....49

Table 11. Coefficients and lack of fit using pentoses and FF response for EC.....50

Table 12. Maximum yields of pentoses and FF for SBS.....52

LIST OF ACRONYMS AND ABBREVIATIONS

CBMM	Companhia Brasileira de Metalurgia e Mineração
CL	Catalyst Load
CNPEM	National Center for Research in Energy and Materials
CONAB	Companhia Nacional de Abastecimento
CrI	Crystallinity Index
EC	Energy Cane
EDS	Energy-Dispersive X-ray spectroscopy
ELSD	Evaporative Light Scattering Detector
FAOSTAT	Food and Agriculture Organization of the United Nations
FCCD	Faced Centered Composite Central Design
FF	2-furfuraldehyde
HMF	5-hydroxymethyl-2-furfuraldehyde
HPLC	High-Performance Liquid Chromatography
LB	Lignocellulosic Biomass
NbP	Niobium Phosphate
NREL	National Renewable Energy Laboratory
PDA	Photodiode Array
SBS	Sugarcane Biomasses
SCB	Sugarcane Bagasse
SCS	Sugarcane Straw
SEM	Scanning Electron Microscopy
T	Temperature
t	Time
UV	Ultra-Violet
XRD	X-Ray Diffraction

LIST OF SYMBOLS

%	Percentage
°C	Degree Celsius
θ	Theta

SUMMARY

1. INTRODUCTION 12
2. LITERATURE REVIEW 14
   2.1 Biomass and biofuel 14
   2.2 Sugarcane as source of lignocellulosic biomass 18
      2.2.1 Energy cane 21
   2.3 Lignocellulosic biomass pretreatment 23
      2.3.1 Physical pretreatments 24
      2.3.2 Chemical pretreatment 25
      2.3.3 Physico-chemical pretreatment 26
      2.3.4 Hydrothermal solid catalyst pretreatment 27
   2.4 Niobium phosphate 29
   2.5 Furfural 31
3. MATERIALS AND METHODS 33
   3.1 Chemicals and materials 33
   3.2 Biomasses preparation 33
   3.3 Catalyst preparation 34
   3.4 Design of experiments 34
   3.5 Pretreatment 35
   3.6 Liquor analysis 36
   3.7 Cellulignin analysis 36
4. RESULTS 37
   4.1 Characterizations 37
   4.2 Pretreatment 41
   4.3 Statistical analysis 46
   4.4 SCB cellulignin characterization 52
      4.4.1 x-ray diffraction 52
      4.4.2 Screening electronic microscopy and Energy-Dispersive x-ray Spectroscopy 53
5. CONCLUSION 56
6. REFERENCES 57

1. INTRODUCTION

Concerns about fossil fuel availability and the increase in energy demand over the rise of the human population have been global issues (HARAHAP, 2020). In addition, using fossil fuels as an energy source is associated with environmental problems (e.g., greenhouse gases) and health problems due to secondary particulates (LOTT, PYE; DODDS, 2017). Thus, alternative fuels, such as lignocellulosic biomass, have been demonstrated as a potential alternative material (HARAHAP, 2020). Lignocellulose biomass is an abundant renewable resource that comprises three major components, cellulose, hemicellulose, and lignin (HARAHAP, 2020; JÖNSSON; ALRIKSSON; NILVEBRANT, 2013). The cellulose and hemicellulose can be hydrolysate in monosaccharides used as fermentation substrates to produce biofuels and biochemicals (HARAHAP, 2020).

Lignocellulosic feedstock includes residues from biorefineries, agriculture, and forestry. The fuel obtained from these materials is often called second-generation fuel. This fuel category avoids the dilemma of fuel-versus-food of first-generation fuel (e.g., bioethanol by fermentation of sugarcane juice) (NAIK et al., 2010).

A great opportunity relies on the residues of the ethanol/sugar industry. According to the Companhia Nacional de Abastecimento (CONAB), 596 million tons of sugarcane are estimated as a 2022/2023 crop in Brazil. Approximately 27.5% and 14% of sugarcane refer to bagasse and straw, respectively (FORMANN et al., 2020). However, the natural recalcitrance of lignocellulosic material becomes an obstacle to converting biomass into biofuel or biochemical (ZOGHLAMI; PAËS, 2019). Removing hemicellulose is an essential step to overcoming this obstacle since it acts as a physical barrier limiting the accessibility of enzymes (ZOGHLAMI; PAËS, 2019).

There are many examples of pretreatments with different objectives and conditions (RUIZ, THOMSEN; TRAJANO, 2017). The pretreatments commonly used are autohydrolysis, using acids, and steam explosion, when the goal is to increase enzymatic digestibility by removing hemicellulose (RUIZ; THOMSEN; TRAJANO, 2017). However, hydrothermal pretreatments require high temperatures and high pressures, and acid pretreatments produce equipment corrosion (RUIZ; THOMSEN; TRAJANO, 2017). Solid catalysts are an excellent substitute for mineral acid in pretreatments since they decrease temperature and pressure and avoid corrosion (VILCOCQ et al., 2014).

Solid catalysts can be safe and non-corrosive beyond that easily recoverable. Solid acid catalysts can be classified into zeolites, resins, carbon material, heteropoliacids, and metal

oxides or phosphates (VILCOCQ et al., 2014). A promising catalyst for biomass valorization is niobium phosphate (NbP) (CAMPISI et al., 2018; CATRINCK et al., 2020; GÓMEZ BERNAL; BERNAZZANI; RASPOLLI GALLETTI, 2014; KANG et al., 2021). NbP is a white powder and water-tolerant catalyst combining Lewis and Brønsted acid sites (KANG et al., 2021). The Brønsted acid sites of NbP are due to P-OH and Nb-OH, whereas Lewis acid sites are associated with the unsaturated Nb^{5+} (GÓMEZ BERNAL; BERNAZZANI; RASPOLLI GALLETTI, 2014). Lewis and Brønsted acid sites are involved in biomass reactions.

The Brønsted acid sites act in biomass hydrolysis, breaking the ether bonds between two monomer sugars and the dehydration of xylose of furfural (CHEN; LEE, 2020). The dehydration process of Brønsted acid sites occurs in a direct path, whereas Lewis acid sites are by the isomerization of xylose in xylulose and lyxose, then using Brønsted acid to dehydrate to furfural (CHOUDHARY; SANDLER; VLACHOS, 2012). Despite the NbP having both acid sites, Brønsted sites are prevalent over Lewis sites with strong acid properties (CATRINCK et al., 2020). Thus, a further study of the release of pentoses and formation of furfural using NbP as the catalyst is required. A statistical approach was performed by using a face-centered composite design (FCCD), with temperature, catalyst load, and time as variables. This work intends to provide comprehensive knowledge of the pentoses and furfural behavior over time in different conditions with different biomass. Thus, obtaining the maximum yields of furfural and xylose by hemicellulose solubilization.

2. LITERATURE REVIEW

2.1 Biomass and biofuel

Over the years, the population worldwide has been increasing. The current population corresponds to twice the population of 1960; even further, in the year 2050 is an estimated growth of 9 billion (PEREA-MORENO; SAMERÓN-MANZANO; PEREA-MORENO, 2019). As the population increases, the global demand for energy increases as well. Throughout history, the early energy source was the direct combustion of wood. However, the main energy source changed with the industrial revolution, as shown in Figure 1 (AKIA et al., 2014; PEREA-MORENO; SAMERÓN-MANZANO; PEREA-MORENO, 2019).

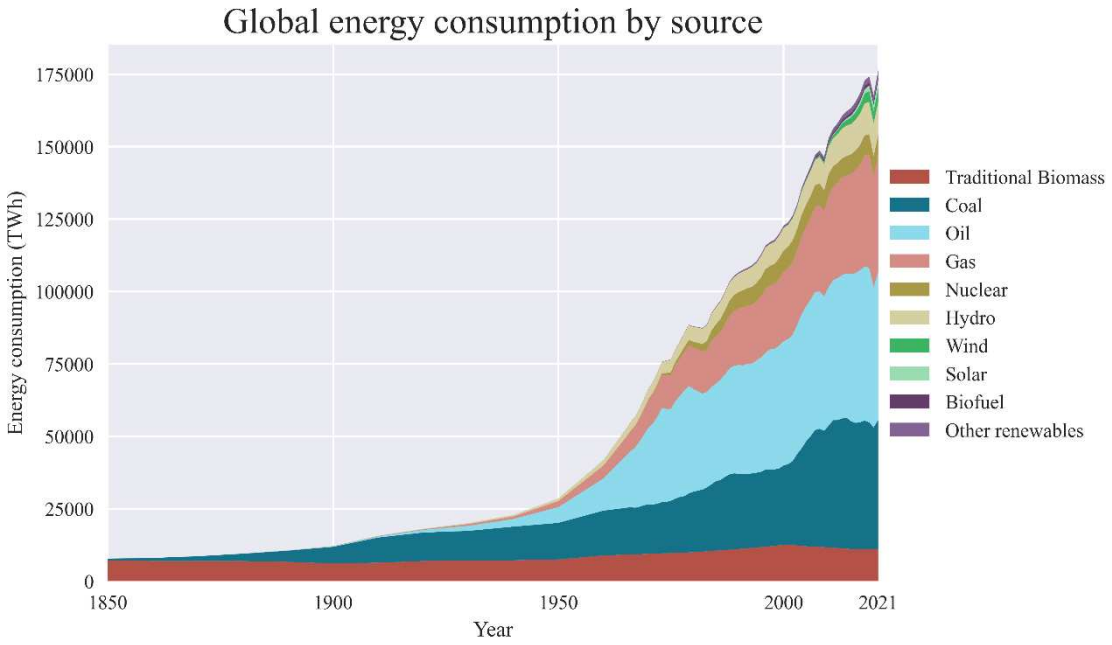

Figure 1 World energy consumption by source over the years 1850 to 2021 (Data source: (OUR WORLD IN DATA, 2021)).

Since then, fossil fuels have had a greater share of the world's energy demand. According to the International Energy Agency report, fossil fuels represent 81% of all fuel used in 2018 for primary energy. However, this number tends to drop over the years, and in 2040 is estimated to be 74% of fossil fuel energy ("International Energy Agency", 2019). Despite the percentage decrease, it is still a significant concern, primarily for the environment. Global warming and air pollution are some problems caused by using fossil fuels that directly impact the health and quality of life of populations (MARTINS et al., 2019). In addition, fossil fuels are not renewable, and eventually, there will decrease, going against the rising energy demand trend. Thus,

other sources of energy should be implemented to substitute and eventually replace fossil fuels (TURSI, 2019).

Among all alternatives, *e.g.,* solar, wind, geothermal, and nuclear, biomass represents a promising renewable and reliable energy source. Biomass, by definition, is the matter of all living organisms in the biosphere, including animals, plants, and microorganisms (HOUGHTON, 2008; PEREA-MORENO; SAMERÓN-MANZANO; PEREA-MORENO, 2019). This source type can be extremely beneficial in some aspects compared to fossil fuels. As a renewable source, biomass can be replenished and will not terminate. In addition, a home-produced source of energy can relieve the reliance on imported fuel and avoid the price change over political issues or demand (NIGAM; SINGH, 2011; PEREA-MORENO; SAMERÓN-MANZANO; PEREA-MORENO, 2019). Also, biomass can reduce greenhouse gas emissions. Even though biomass releases almost the same amount of CO_2 during combustion, that, during its growth, capture the CO_2 emitted. Thus, the overall process is a zero-net balance of CO_2 emission (HOUGHTON; NATIONAL RENEWABLE ENERGY LABORATORY; HOUGHTON, 2008; PEREA-MORENO; SAMERÓN-MANZANO; PEREA-MORENO, 2019; TURSI, 2019).

Biomass comprises various materials, including agricultural, animal, and forestry products and waste (TURSI, 2019). The most common biomass materials for biofuel production are forest and agricultural. These biofuels are often divided into primary and secondary; the secondary biofuel is separated by generations. Primary biofuel uses an unprocessed form of biomass, such as combustion for heating, cooking, or electricity. This kind of fuel was the primordial type until the use of fossil fuels in the industrial revolution (NIGAM; SINGH, 2011; OUR WORLD IN DATA, 2021). The secondary biofuels use modified primary biofuels obtained from these solid (charcoal), liquid (bioethanol), or gas (butane) fuels (NIGAM; SINGH, 2011).

The secondary biofuel can be divided into four generations (Figure 2). The first generation is based on biofuel from edible feedstocks, including rice, sugarcane, seeds, potato, and other vegetables. These feedstocks undergo a fermentation process for ethanol production or a transesterification process for biodiesel production (MAT ARON et al., 2020; NIGAM; SINGH, 2011). Although a great success in biofuel, the first-generation biofuel has a downside; the fuel source is derived from food and requires certain amounts of land area and water supply (ZOGHLAMI; PAËS, 2019). The "food vs. fuel" dilemma allied with some kinds of biofuels producing negative net energy gain, which lead to more greenhouse gases in the production stage, made a necessary shift (MAT ARON et al., 2020; ZOGHLAMI; PAËS, 2019).

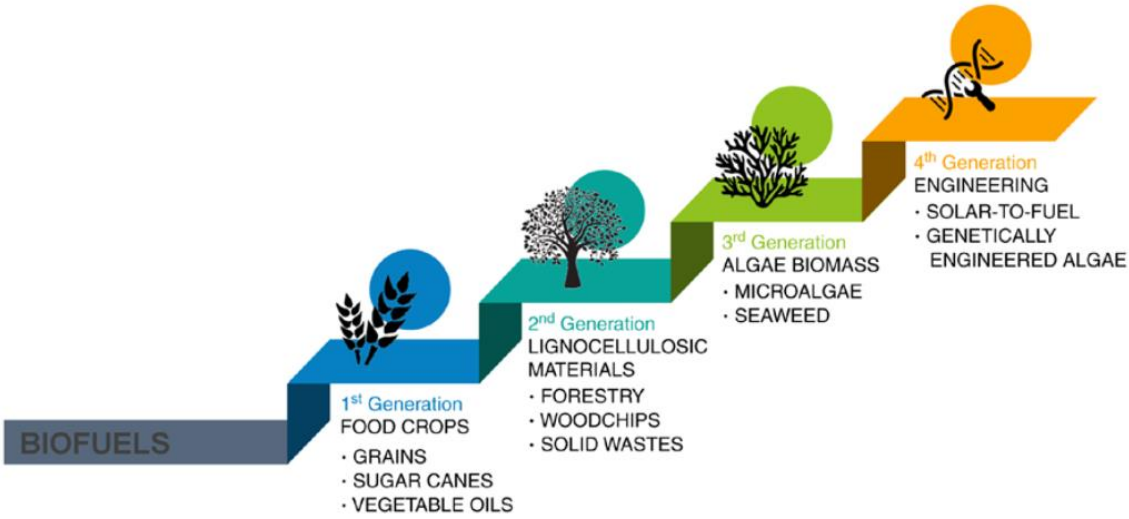

Figure 2 Generations of biofuels according to source and process.(PAPAKONSTANTINOU et al., 2021)

Second-generation biofuels arrived to overcome the downsides of first-generation, mainly the "food vs. fuel" dilemma. The difference between the two generations is the feedstock. Second-generation biofuel uses non-edible biomass, primarily waste from crops and forestry. This characteristic results in significant advantages. The most evident is the lack of food competition, requiring no more specific land areas or other agricultural supplies since only waste is used (MAT ARON et al., 2020). As for greenhouse gases, second-generation produce fewer gases than different generations. Bioethanol produced by agricultural and forestry waste is estimated to reduce 70-85% of greenhouse gases (GNANSOUNOU, 2010).

The agricultural and forestry biomasses are often called lignocellulosic biomass (LB). LB has three principal components, cellulose, hemicellulose, lignin (Figure 3), and other components in minor quantities, such as minerals and acetyl groups (ISIKGOR; BECER, 2015; LIU et al., 2022). The proportion of these components varies according to the plant (TURSI, 2019).

Cellulose is the most abundant biopolymer in nature and the primary component in LB. The cellulose chain consists of units of dimers called cellobiose, which comprise two D-glucose linked by B-1-4 glycosidic bonds (ISIKGOR; BECER, 2015; TURSI, 2019). This organization allows extensive intramolecular and intermolecular hydrogen bonding, creating closer bonds between glucose units (ISIKGOR; BECER, 2015). These intramolecular and intermolecular bonds increase the polymer's stability and rigidity, creating an orderly crystalline region (TURSI, 2019).

Hemicellulose is a biopolymer based on branched polysaccharides heterogeneously mixture composed of glucose, xylose, and arabinose (ISIKGOR; BECER, 2015; ZOGHLAMI; PAËS, 2019). Usually, hemicellulose comprehends the second principal component in LB and,

therefore, the second most abundant polymer in nature (ISIKGOR; BECER, 2015). The random disposition of the heteropolymers promotes an amorphous structure. The composition and disposition of the carbohydrates in LB depend on the type and species of the plant (ISIKGOR; BECER, 2015).

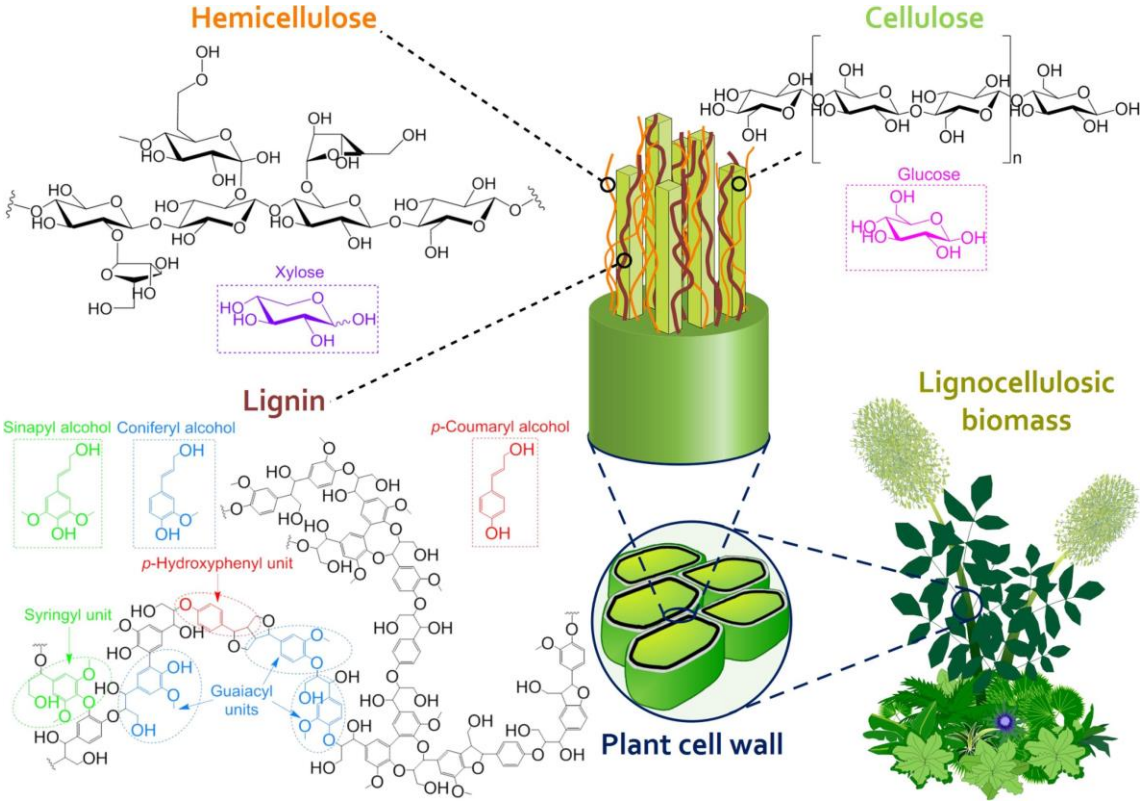

Figure 3. The general structure of lignocellulosic biomass and its components.(SOLTANIAN et al., 2020)

Lignin is a three-dimensional complex amorphous polymer composite of phenylpropanoid monomeric units. The linkage between monomeric units can occur through oxygen bridges or carbon-carbon bonds between the same groups. The lignin acts as a cement or glue, putting the fibbers of LB together; this conformation ensures the plant structure resistance (ISIKGOR; BECER, 2015; TURSI, 2019). The content of lignin content varies by species and age (TURSI, 2019).

The main biorefinery issue is the recalcitrance nature of the complex mixture of the three major LB components. Pretreatment is generally used according to the process's objective to overcome this problem (BHATIA et al., 2020).

The third-generation biofuel aims to produce biochemical using mainly algae-derived as an energy source (PAPAKONSTANTINOU et al., 2021). Algae-derived biomass consists of lipids, carbohydrates, and protein molecules (PAPAKONSTANTINOU et al., 2021). The algae are usually classified into two groups based on morphology and size, macro-algae and micro-

algae. Microalgae have great potential to produce biochemicals with less space required, high oil content, and the ability to endure various growth conditions (ALALWAN; ALMINSHID; ALJAAFARI, 2019; PAPAKONSTANTINOU et al., 2021). Despite all the advantages, biofuel from algae does not show economically viable costs compared to fossil fuels (PAPAKONSTANTINOU et al., 2021).

The fourth biofuel generation is still in the early stages of research and experiments. The feedstock used in this generation is biomass genetically engineered. This biomass is genetically modified to produce low lignin and cellulose content, less recalcitrance (second-generation issue), or increasing oil or lipids in algae improving third-generation biofuels (ZIOLKOWSKA, 2020). The fourth generation can also improve CO_2 sequestration, leading to a more eco-friendly source (PAPAKONSTANTINOU et al., 2021).

2.2 Sugarcane as source of lignocellulosic biomass

Sugarcane is the most produced agricultural commodity worldwide, representing 21% of the total production of crops in the year 2019, according to the Food and Agriculture Organization of the United Nations (FAOSTAT)(FAO, 2021). The production is concentrated in tropical areas between 30° of latitude, as shown in the map (Figure 4.A)(NEGRÃO et al., 2021). Brazil occupied first place in the sugarcane harvest, followed by China and India. Figure 4.B shows the yield, area, and production (bubble size) of the main countries in sugarcane crops.

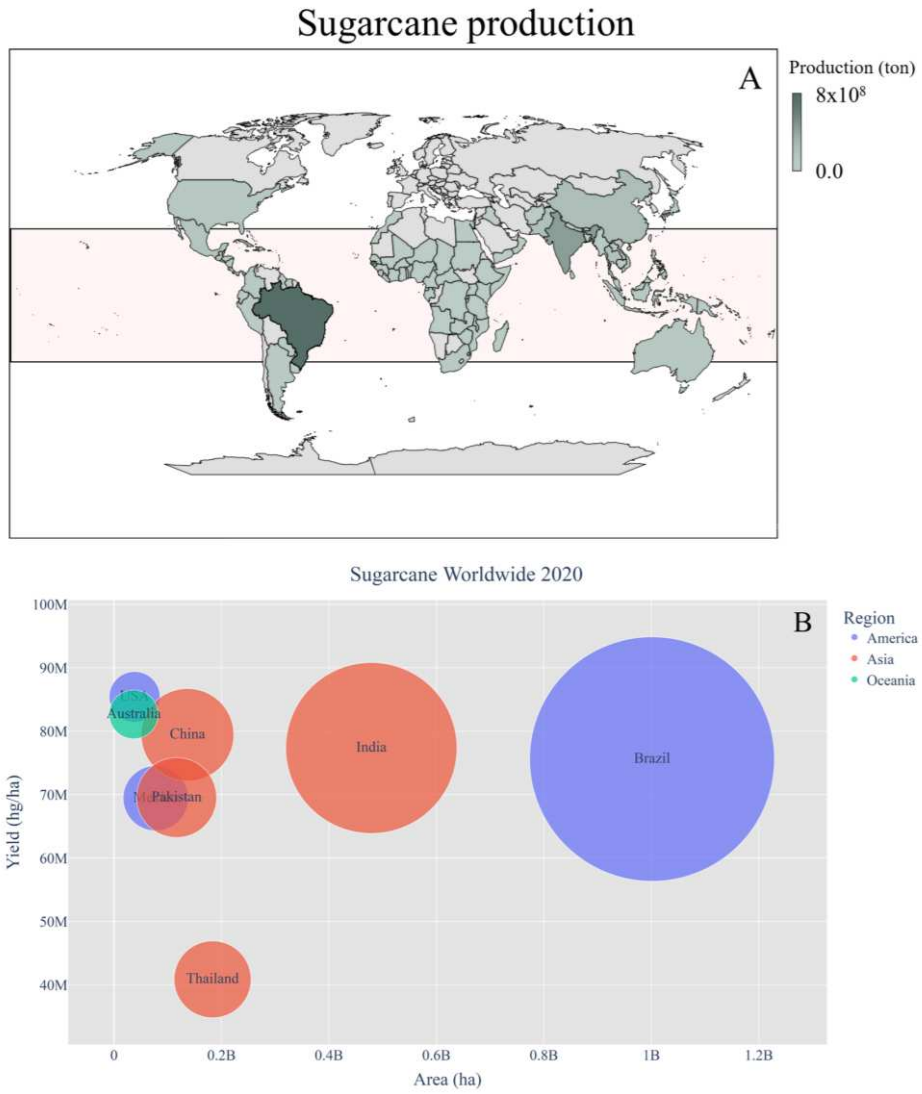

Figure 4 . Sugarcane production worldwide map (a) and leading countries in sugarcane production with respective yield, area, and production (bubble size) (b). (Data source: (FAO, 2021))

Inside Brazil, sugarcane production is distributed, as the map in Figure 5.A shows. Above is shown the map (Figure 5.A) based on sugarcane production, and below is the map based on ethanol and sugar plants (Figure 5.B) (COMPANHIA NACIONAL DE ABASTECIMENTO, 2022; NOVACANA, 2022).

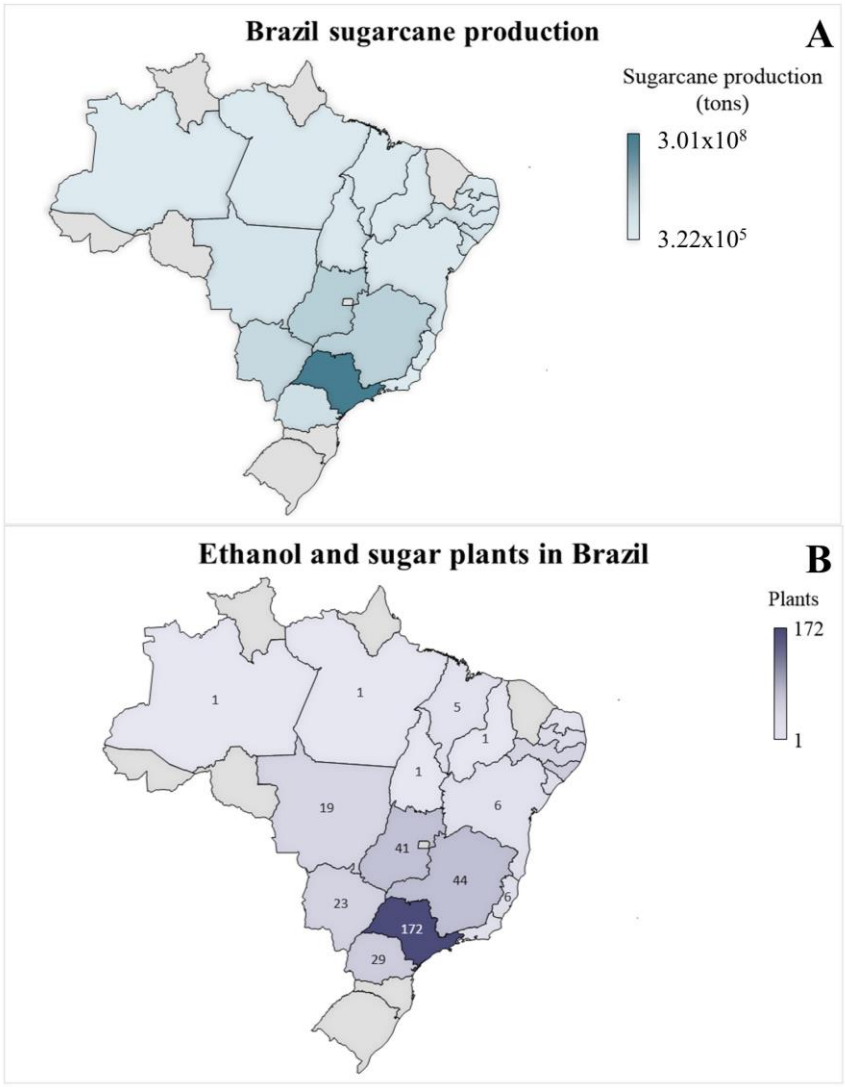

Figure 5 . Brazil map of sugarcane production for each state (A) and Brazil map of sugar and ethanol plant for each state (B). (Data source: (COMPANHIA NACIONAL DE ABASTECIMENTO, 2022) (a), NovaCana(NOVACANA, 2022) (b)).

The ideal situation is an integration of second-generation on a well-established first-generation ethanol plant. The number of plants shown in Figure 5.B, could scale up ethanol production by integrating second-generation fuel and minimize the capital investment if compared with stand-alone second-generation. On an environmental level, the integration also is beneficial since the biomass will be more extensive and intensively used. However, some drawbacks turn this process not economically available yet. An example is the difficulty of obtaining a high sugar concentration and a low inhibitor concentrationn the pretreatment step (AYODELE; ALSAFFAR; MUSTAPA, 2020; DIAS et al., 2014).

Since the 1980s, Brazil has been producing large-scale bioethanol first-generation. Therefore, a large amount of sugarcane biomass is produced, divided into parts (NICULA DE CASTRO; BRITO ALVES; OLLER NASCIMENTO, 2021). The generic structure of the sugarcane plant is shown in Figure 6. The top and the leaves are grouped and defined as straw. From the stalk is removed the juice, rich in sugars, and the dry stalk fiber is called bagasse (NEGRÃO et al., 2021).

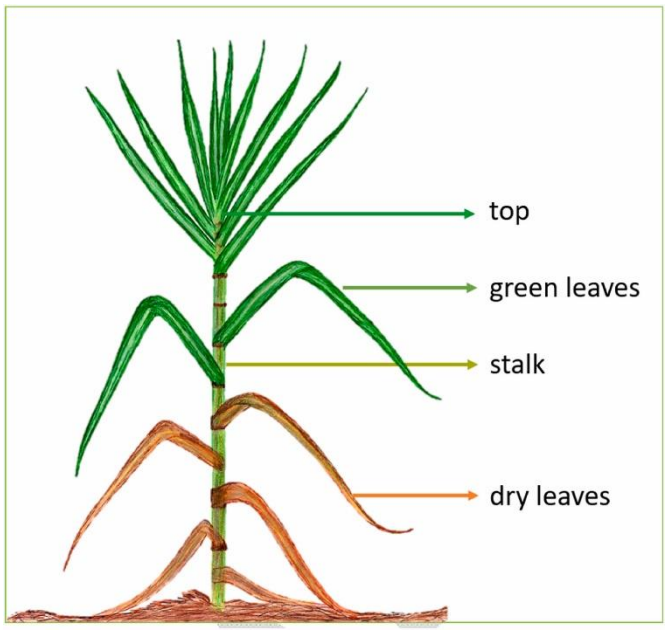

Figure 6 Depiction of sugarcane plant and its fractions(NEGRÃO et al., 2021).

The chemical composition of sugarcane bagasse and sugarcane straw varies depending on several factors, such as plant genetics, growth environment, and process conditions. The method applied for characterization also can influence the result. Therefore is hard to compare biomasses of different origins or characterized in different laboratories (CANILHA et al., 2012). The sugarcane bagasse is composed of 38-45.5% of cellulose, 22-27% of hemicellulose, and 17-33% lignin, whereas sugarcane straw is composed of 33-39% of cellulose, 18.4-28.9% of hemicellulose, and 21.5-40% lignin (CANILHA et al., 2012; COSTA et al., 2013; DA SILVA et al., 2010; GUILHERME et al., 2015; LALUCE et al., 2019; LUZ et al., 2010; ROCHA et al., 2015; SAAD et al., 2008).

2.2.1 Energy cane

Usually, the main objective of sugarcane cultivation is to increase sugars in the stalks. However, the research and development for second-generation biofuels using LB as a feedstock source, has grown an interest in the sugar and the fibers (DE ABREU et al., 2020). Alexander, with his group, has already seen this trend. They said in 1985 that the evaluation of sugarcane

quality was not measured only by the sugar content; sugarcane is an instrument of growth, a producer of biomass unequaled. From that, the term "energy cane" (EC) surged, with a concept of management that the goal was to produce more biomass (MATSUOKA et al., 2014).

The difference between the traditional sugarcane and EC can be visually observed. In general, EC has a narrow leaf blade, a thinner stalk, and a more profuse tillering (MATSUOKA et al., 2014). Table 1 shows the sugarcane cultivation difference between the common sugarcane and the EC. The main difference is the fiber content, which EC has 10% more fiber (GRASSI; PEREIRA, 2019).

Table 1 Compares sugarcane and energy cane (GRASSI; PEREIRA, 2019).

	Sugarcane	**Energy Cane**
Fiber	17.4%	27.0%
Total sugars	12.6%	8.5%
Productivity (tonne/ha)	92	180
Use of fertilizes	2%	5%
Biotic and abiotic stress resistance	Low	Medium
Number of harvests	5	10

Abreu et al., 2020 studied the growth of sugarcane (*Saccharum spp.*) and the EC exploring the sprouting process. The growth model is shown in Figure 7. As shown in Figure 7, the sugar contents as the physical characteristics. The EC presents low sugar contents with early development, suggesting that the EC may start the photosynthesis process very early. Abreu et al., 2020 concluded that EC has a higher sprouting rate, followed by a rapid shoot development and later formation of roots (DE ABREU et al., 2020).

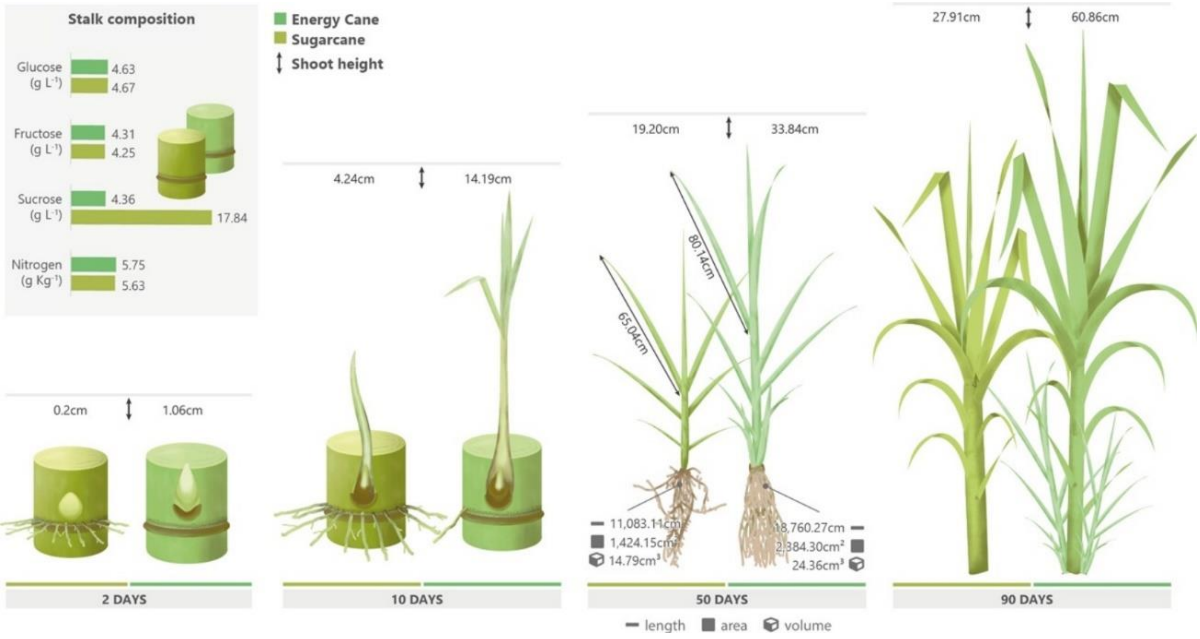

Figure 7 Representation of the development of sugarcane and energy cane (DE ABREU et al., 2020).

2.3 Lignocellulosic biomass pretreatment

The complex structure of LB components, called recalcitrance, has been the main issue in biorefinery. LB recalcitrance provides resistance against physical, chemical, and biological attacks on the plant. This resistance prevents microbial and enzymatic degradation of LB and therefore prevents sugar release and fermentation (BHATIA et al., 2020; ZOGHLAMI; PAËS, 2019). Many factors contribute to the recalcitrance of LB, such as the degree of polymerization of cellulose, acetylation of hemicellulose, interactions between polymers, and lignin acting as a physical barrier (ZOGHLAMI; PAËS, 2019).

A step between feedstock and saccharification or fermentation process is necessary to overcome this issue. This step is called pretreatments. Several pretreatments can be categorized into groups, such as physical, chemical, physical-chemical, biological, and combined. Figure 8 illustrates some pretreatments and their groups (SOLTANIAN et al., 2020).

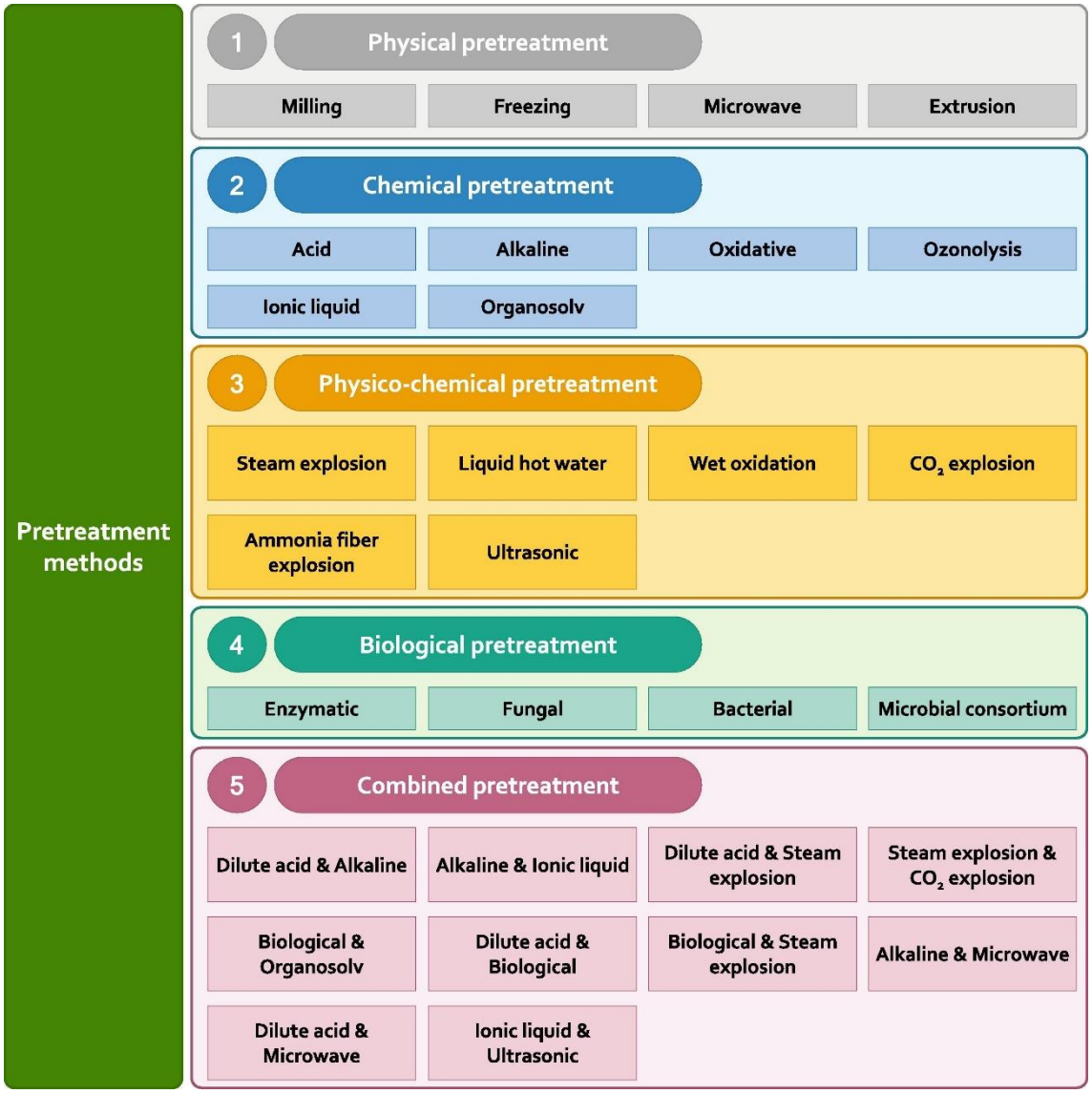

Figure 8 Classification of different types of pretreatment methods for lignocellulosic biomass (SOLTANIAN et al., 2020).

Pretreatment is a crucial step in biofuel production, which requires high capital, high chemical or/and energy consumption, and significant operational and logistics (SOLTANIAN et al., 2020). These characteristics make pretreatments the most expensive process in the conversion of LB (CHEAH et al., 2020). In general, the pretreatment objectives comprise: *i*) obtain higher sugars yields, *ii*) be viable to all LB, *iii*) remove or break specific LB components, *iv*) minimize energy and operation costs, and *v*) value the LB and its byproducts (CHEAH et al., 2020).

2.3.1 Physical pretreatments

The physical pretreatment process has the main objective the LB particle size reduction. Examples of physical pretreatment are milling, extrusion, microwave, and freezing, as shown

in Figure 8. In this process, mechanical tools and techniques such as millers, grinders, and microwaves are usually used. **Table 2** shows some advantages and disadvantages of certain physical pretreatments (MANKAR et al., 2021; SOLTANIAN et al., 2020).

Table 2 Advantages and disadvantages of physical pretreatments. (Soltanian et al., 2020).

Physical pretreatment	Advantages	Disadvantages
Milling	• Reduce particle size and cellulose crystallinity • Improve LB available surface for the enzymatic process • No inhibitors are formed	• High energy consumption • Lignin is not removed • The digestibility of enzymes is limited.
Extrusion	• Low cost • Good mixing • No inhibitors are formed • Simple process	• The digestibility of enzymes is limited. • High energy consumption
Freezing	• No inhibitors are formed • Increase in glucose accessibility • Increase in enzyme digestibility	• High-cost process
Microwave	• High heating efficiency • Simple process • Degradation of LB structure	• High energy consumption • High investment required • Formation of some inhibitors

2.3.2 Chemical pretreatment

Using chemical substances such as acids, alkalines, or organic solvents characterizes chemical pretreatments. The most common pretreatments are acid and alkaline-catalyzed (MANKAR et al., 2021). These pretreatments are the most applied method on large and commercial scales (CHEAH et al., 2020). Figure 8 shows examples of chemical pretreatments.

Acids pretreatment has the main objective of removing the hemicellulose fraction of LB. In this process, the acid acts as a catalyst by rapidly protonating the oxygen atom, followed by a breakdown of the glycosidic bond and forming a carbocation which will add a water molecule (RUIZ; THOMSEN; TRAJANO, 2017). The most common acids used in this pretreatment are

diluted mineral acids (sulphuric, nitric, hydrochloric acid) and acetic acid (CHEAH et al., 2020; MANKAR et al., 2021). This process occurs in mild temperatures in a relatively short time (1-90 minutes). However, the use of acid leads to a high inhibitors generation such as 5-hydroxymethyl-2-furfuraldehyde (HMF), and 2-furfuraldehyde (FF), besides required neutralization and high-cost acid-resistant reactors.

Alkaline pretreatment mainly aims to solubilize lignin from LB and is often used in the paper industry (GALBE; WALLBERG, 2019). The pretreatment uses alkaline compounds such as potassium, sodium, ammonium, and calcium hydroxides as catalysts. The accessibility of enzymes is improved since the lignin carbohydrate complex bonds (ester, aryl-ether, alkyl-aryl) will be cleavaged. These reactions occur via saponification and solvation, and then acetyl groups and uronic acids are removed from the hemicellulose (MANKAR et al., 2021). This pretreatment shows less sugar degradation, is made at relatively low temperature, and improve enzymatic digestibility. However, it presents a high inhibitor concentration, is high-cost processing, and just as acid pretreatment needs to be neutralized (MANKAR et al., 2021; SOLTANIAN et al., 2020).

2.3.3 Physico-chemical pretreatment

Physico-chemical pretreatments combine physical and chemical, i.e., milling and acid pretreatment (CHEAH et al., 2020). Figure 8 shows examples of physicochemical pretreatments; of the ones presented, steam explosion and liquid hot water are the most common (BRODEUR et al., 2011). In both cases, the only chemical used is water with high temperatures (GALBE; WALLBERG, 2019).

The steam explosion pretreatment process is quite simple. The LB is exposed to high-pressure steam followed by a rapid pressure release (CHEAH et al., 2020). This fast change in pressure disrupture the fibrils and increase the cellulose accessibility (BRODEUR et al., 2011). During the process, the main effects that influence the pretreatment result are the time, pressure, the release rate of the pressure, and the effect caused by shearing between the chips (GALBE; WALLBERG, 2019). Studies show that steam explosion positively increases the LB's porosity without disintegrating the wood (GALBE; WALLBERG, 2019). Despite the increase in hemicellulose and lignin solubilization, this process forms inhibitors and incomplete hemicellulose degradation (SOLTANIAN et al., 2020).

Liquid hot water is a pretreatment where the LB is mixed with only water and heated to 150 – 220°C at high pressure. The main objective of this process is to remove the hemicellulose. This process is considered eco-friendly since no other reagent is needed. When the water

reaches high temperatures under pressure the hydrogen bonding starts to weaken increasing the concentration of hydronium and hydroxide ions. These ions participate as acid or basic catalysts in hemicellulose removal (RUIZ, THOMSEN; TRAJANO, 2017). This process generates a carbohydrate-rich liquor and a solid fraction containing cellulose and lignin. Besides the high recovery of sugars, hot liquid water pretreatment is a high-cost process, demanding a large amount of water and high energy consumption (SOLTANIAN et al., 2020).

2.3.4 Hydrothermal solid catalyst pretreatment

A solid catalyst can be used to overcome hydrothermal pretreatment's high-cost process. Solid catalyst presents several advantages if compared to simple acid pretreatment. These catalysts can be easily recovered since they are heterogeneous, can be reused, and are safe and non-corrosive. Thus, the major problems of acid pretreatment are avoided, and the advantages of these pretreatments are (VILCOCQ et al., 2014).

The term heterogeneous catalyst can describe a wide range of catalysts. The ones usually applied in LB pretreatment can be classified as zeolites, resins and polymers, carbon materials, oxides/phosphates, and others. Each group of catalysts presents characteristics such as surface area and acid sites (VILCOCQ et al., 2014).

Zeolites comprehend a complex tridimensional structure of crystalline aluminosilicates. Stability-wise, zeolites are questionable and can be deactivated around 200°C in a water medium. The main characteristic of zeolites catalyst is the Si/Al ratio. The increase in this ratio decreases the Bronsted acid sites and increases the average acid strength (VILCOCQ et al., 2014). Yoshida et al., 2014, tested four types of zeolites with different Si/Al ratios, 7, 20, and 10. The experiments were carried out using bamboo in high temperatures and time predetermined. In conclusion, Yoshida et al., 2017 showed that in 1h, the best zeolite, Faujasite-type Si/Al of 20, converted the most hemicellulose and produced the highest concentration of furfural (YOSHIDA et al., 2017).

Resins and polymers are solid with polymer-based composition, usually with sulphonic groups (SO_3H), giving the Bronsted acid characteristic. A widely used resin is Amberlist-15; it presents a structure of a styrene-divinylbenzene polymer with ion exchange proprieties (DENG et al., 2022; VILCOCQ et al., 2014). However, Amberlyst-15 resin does not stand at temperatures higher than 120 °C; even the most temperature-resistant resin, Amberlyst-45, can not stand more than 170°C (DUPONT, 2022). Siril et al., 2008 have studied four types of Amberlyst resins, Amberlyst 70, Amberlyst 15, Amberlyst 35, and Amberlyst 36. In this study, Siril et .al, 2008 showed that for Amberlyst 15 and 35, an increase of temperature to 220 °C has decreased

by approximately 45% in acid sites. In Amberlyst 70, a more temperature resistance resin, a decrease only reach 27%. However, Amberlyst 70 has shown the least amount of acid sites among the resins studied (SIRIL; CROSS; BROWN, 2008). The Amberlyst 70, despite several works, is no longer available to purchase (ANTONETTI et al., 2017b; DUPONT, 2022; HE et al., 2021; LEYVA et al., 2013; SIRIL; CROSS; BROWN, 2008).

Carbon acid catalysts are generally obtained by incomplete carbonization of carbonaceous natural material or by condensation and polymerization of furanic molecules. These materials can be used as metal support or as an acid catalyst (VILCOCQ et al., 2014; WANG et al., 2018). Usually, carbon materials acquire acid properties by sulphonation with fuming sulphuric acid (DENG et al., 2022; VILCOCQ et al., 2014). In biorefineries, carbon materials can be easily prepared by the incomplete combustion of LB or by the hydrothermal approach of dehydrating sugar from hemicellulose to furanic compounds and then polymerizing (hydrochar)(VILCOCQ et al., 2014; WANG et al., 2018). Lu et al., 2021 show the possibility of adding a magnetic characteristic to the catalyst by mixing $FeCl_3$ with cellulose and then carbonization. A magnetic catalyst can easily be recoverable (LU et al., 2021). Bagasse-derived catalyst has shown excellent reusability in esterification reactions in methanol, as described by Lou et al., 2011 with even better results than Amberlyst-15 (LOU et al., 2012). Despite carbon catalysts being very stable in aqueous media, the sulfonated groups can leach during the reaction at high temperatures (VILCOCQ et al., 2014).

Inorganic metal oxides and phosphates are widely used in catalysis due to their porous structure and acid sites. The Lewis acid sites found in these catalysts accelerate sugar dehydration. Meanwhile, Bronsted acid sites contribute to hemicellulose and cellulose hydrolysis (DENG et al., 2022; VILCOCQ et al., 2014). Chareonlimkun et al., 2010 studied the ZrO_2 and TiO_2 with and without sulphonation in the hydrothermal dehydration of sugars. In this case, all catalysts have presented an increase in conversion (CHAREONLIMKUN et al., 2010). The phosphate catalyst was studied by Antonetti et al. 2017 using amorphous NbP and ZrP as catalysts in the fructose dehydration. The reactions undergone in a microwave system contain only water, the substrate, and the catalyst. At 190°C, ZrP had a better selectivity to HMF formation (ANTONETTI et al., 2017[a]). Overall, oxides have demonstrated excellent stability in subcritical and supercritical water conditions, with promising uses in biofuel production (SUDARSANAM; LI; SAGAR, 2020).

2.4 Niobium phosphate

Niobium phosphate or niobium oxophosphate is a heterogeneous acid catalyst with the formula $NbOPO_4.nH_2O$ (ZHU; HUANG, 2009). The use as a catalyst came from NbP having both Lewis and Bronsted acid sites. The Lewis acid sites are attributed to the unsaturated Nb^{5+} cations. The Bronsted acid sites are attributed to the P-OH and Nb-OH, both existing in the NbP surface (KANG et al., 2021). Watered tolerance is the other characteristic that elevates NbP as a catalyst(VIEIRA et al., 2021). The structure of NbP is a connection of the NbO_6 octaedron and PO_4 tetrahedron as an ensemble by sharing the O corner atoms (Figure 9)(KANG et al., 2021).

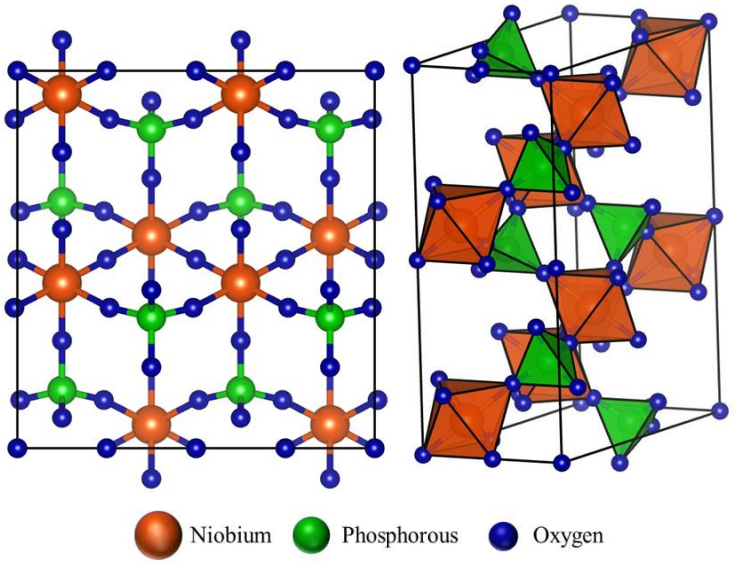

Figure 9. Schematic structure of $NbOPO_4$.

Given all the characteristics, NbP could be a promising catalyst in biofuel production. It is found in literature several papers relating the use of NbP to convert sugars in furanic compounds. (CARNITI et al., 2016; CATRINCK et al., 2020, 2021; CHOUDHARY et al., 2011; CHOUDHARY; SANDLER; VLACHOS, 2012; GÓMEZ BERNAL; BERNAZZANI; RASPOLLI GALLETTI, 2014; VIEIRA et al., 2021). The reason relies on the fact that NbP has both Lewis and Bronsted acid sites. The glucose and xylose conversion paths are shown in Figure 10. The glucose paths to HMF conversion could either directly convert to HMF in a Bronsted-catalysed reaction or by first converting to fructose in a Lewis-catalysed isomerization and then Bronsted-catalysed dehydration (CATRINCK et al., 2020, 2021; VIEIRA et al., 2021). Vieira et al.,2021, have shown a relationship between products to the Lewis/Bronsted acid sites (L/B), in which the reaction rate increase along the L/B. However, if the concentration of Lewis acid sites were too high, compare to Bronsted acid sites, the fructose degradation to

humins (CATRINCK et al., 2020, 2021; VIEIRA et al., 2021). The xylose paths to furfural either directly convert to furfural, by Bronsted-catalysed dehydration or proceed first with a Lewis-catalysed isomerization to xylulose followed by dehydration of xylulose to furfural (Figure 10)(CHOUDHARY et al., 2011). Choudhary et al., 2012 have shown that the combination of Lewis and Bonsted acid has improved substantially the conversion of xylose to furfural in aqueous media (CATRINCK et al., 2020, 2021; CHOUDHARY; SANDLER; VLACHOS, 2012).

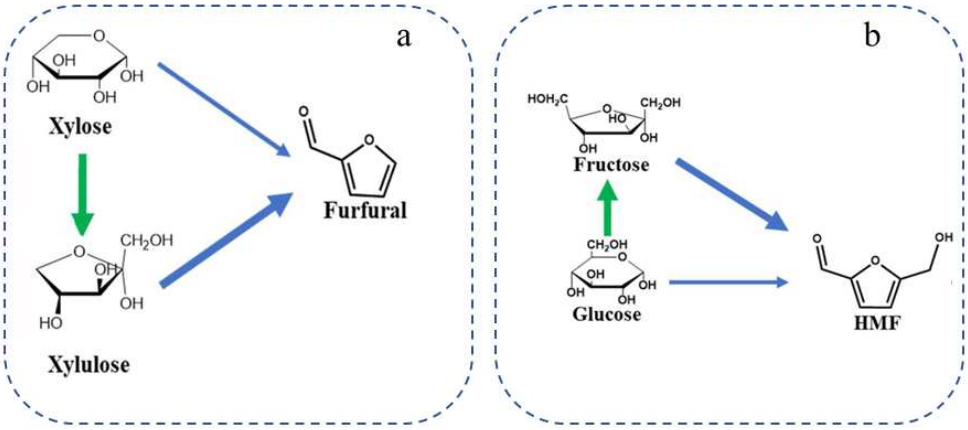

Figure 10 Conversion of xylose (a) and glucose (b) with both Lewis and Bronsted acids. The thicker arrow shows the preferential reaction. The green and blue arrows represent the reactions catalyzed by Lewis and Bronsted acid, respectively.(VIEIRA et al., 2021).

The compositions of synthesized and commercial NbP (by CBMM) are found in a study by Vieira et al., 2021. In this study, different ratios of P/Nb are presented, showing that lower ratios of NbP favor monosaccharide reactions. The lower P/Nb is associated with niobium oxide (VIEIRA et al., 2021). Catrink et al., 2020 characterized both the Lewis and Bronsted acid sites of NbP and niobium oxide provided by CBMM. The results showed that NbP has a ratio of Lewis by Bronsted acid inferior to niobium oxide (CATRINCK et al., 2020).

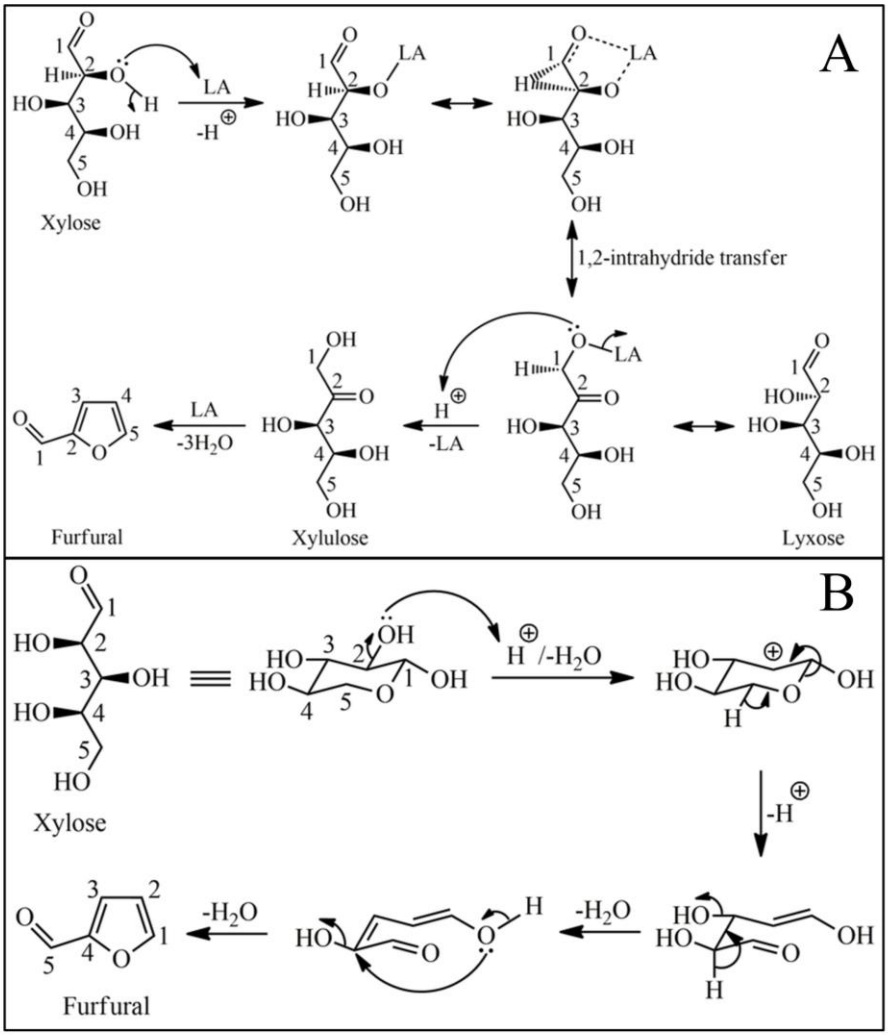

Figure 11. Conversion of xylose to furfural by Lewis acid sites (A) and Bronsted acid sites (B).(BHAUMIK; DHEPE, 2016)

2.5 Furfural

Despite being considered an inhibitor in enzymatic reactions of LB, FF is a promising renewable platform compound. In this case, renewable meaning that can be produced using a renewable source, LB, for example(LI; JIA; WANG, 2016).

According to the U.S. Department of Energy, FF has been considered one of thirty bio-mass-derived molecules(LI; JIA; WANG, 2016). In 2001, 250,000 tonnes of furfural was glob-ally consumed. Usually, FF is commercialized as FF, furfuryl alcohol, or polytetramethylene ether glycol. The FF and its derivations can be used in different areas, as Figure 12 shows.

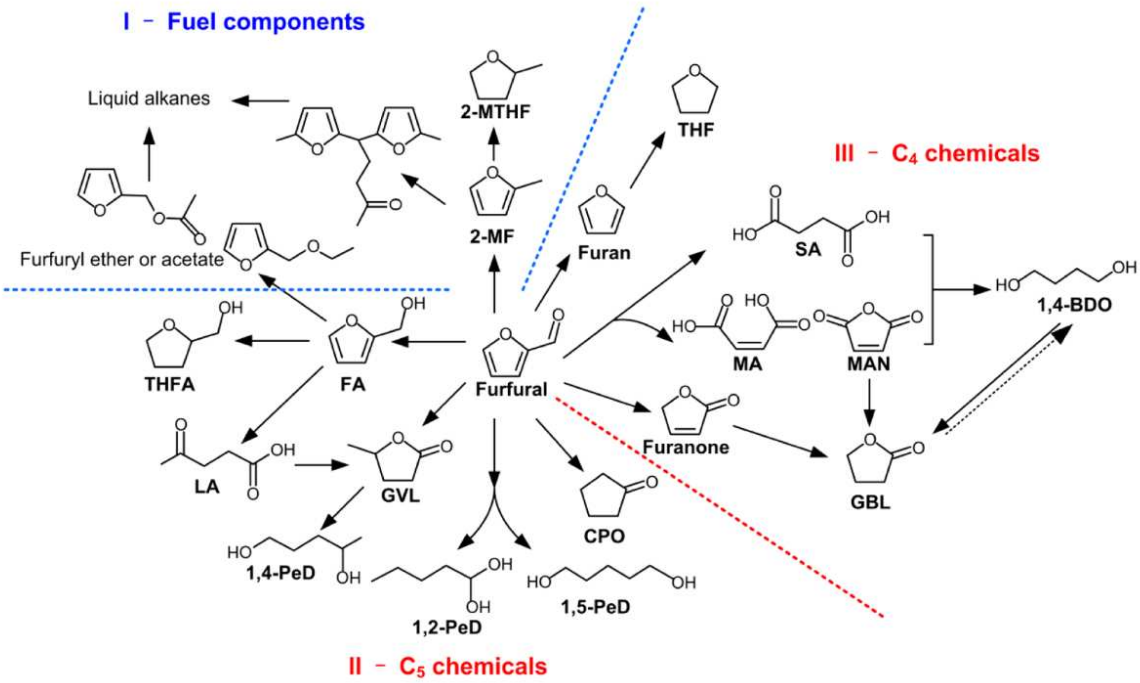

Figure 12 Fuel components and chemicals derived from furfural(LI; JIA; WANG, 2016).

The production of FF is not new and has been produced for over 75 years (KABBOUR; LUQUE, 2020). However, the methods are still traditional and inefficient, reflecting a low FF yield. Thus, producing FF using a catalyst is a promising area to investigate. The uses of heterogeneous catalysts have already been successfully reported, however in many cases using organic solvents (LI; JIA; WANG, 2016).

Table 3. The different processes of furfural production (MARIANA NEVES CATRINCK, 2018).

Substrate	Solvent	Catalyst	T (°C)	t	Conv. (%)	Yield (%)
Xylose	H_2O	None	150	3 h	23.9	3.20
Xylose	H_2O	HCl	160	4 h	35.0	51.0
Xylose	H_2O	Nb_2O_5	120	3 h	93.0	48.0
Xylose	H_2O	Nb_2O_5:$NbOPO_4$	160	30 min	44.1	33.1
Xylose	H_2O	Nb_2O_5-SiO_2/ZrO_2	130	6 h	39.9	23.0
Sugarcane bagasse	H_2O :GVL	Al-Beta	185	85 min	-	51.1
Sugarcane bagasse	H_2O	$NbOPO_4$	150	5 h	-	30.6

3. MATERIALS AND METHODS

3.1 Chemicals and materials

Glucose, xylose, arabinose, 5-hydroxymethyl-2-furfuraldehyde (HMF), and 2-furfuraldehyde (FF) standards were purchased from Sigma-Aldrich (Brazil). Sugarcane bagasse (SCB) and sugarcane straw (SCS) were provided by Laboratório Nacional de Biorrenováveis (LNBR) Campinas (SP), and energy cane (*RB127048*) was provided by the Laboratório de Biotecnolgia e Melhoramento Genético do Departamento de Agronomia da Federal University of Viçosa. EC was used in raw, i.e., juice, bagasse, and straw. Niobium phosphate (NbP) was provided by Companhia Brasileira de Metalurgia e Mineração (CBMM).

3.2 Biomasses preparation

To better identify, all biomasses (SCB, SCS, and CE) will be referred to as sugarcane biomasses (SBS).

Before the characterization and the pretreatment, the SBS was washed several times to remove extractives in the biomass. First, 15g of SBS was washed eight times with 300 mL of distilled water at 70°C, followed by six times with 250 mL of ethanol at 70°C. The washed SBS was dried in a recirculation oven for 24 hours at 70°C. Samples of the SBS washed were taken to verify the moisture content. The moisture was kept below 10% to avoid biological degradation.

The dried SBS were grounded in a Thomas Scientific model 4 knife mill. The granulometry analysis was made by using different mesh sieves. In a sieve shaker were placed 20, 35, 48, 65, and 80 mesh sieves piled, and on top of 20 mesh sieves was placed 200 g of ground SBS. After 30 minutes, the content of each sieve was weighed.

The moisture content was determined by a BEL Engineering i-Thermo G163M moisture analyzer. Approximately 1 g of SBS was placed in the moisture analyzer and then heat until the weight stabilized. The instrument was set at a temperature of 105 °C, without pre-heating, and with a rate of 0.1 % per minute. All the analyses were made in triplicate.

The carbohydrates and lignin composition of the SBS were made by the Laboratório de Celulose e Papel from the Federal University of Viçosa. These analyses were performed according to SCAN-CM 71:09, Tappi T 222om-98, and T 264 cm-97 methods. The ashes were quantified following the procedure provided by the National Center for Research in Energy and Materials (CNPEM). In this procedure, the crucibles were heated in a muffle for 3 h at 800°C. After reaching room temperature, approximately 2g of SBS were placed in the crucibles

previously weighed. The calcination was made in three stages, the first stage was 1h at 200 °C, the second stage was 1 h at 400 °C, and the last stage was 2 h at 800°C. After cooling down, the crucibles with the ashes were weighed and then determined by Equation 1.

$$Ashes = \frac{m_{tac} - m_c}{m_s} \times 100 \qquad \textbf{Equation 1}$$

where m_{tac} is the mass of total ashes plus the crucible, m_c is the mass of the crucible, and m_s is the mass of the dry sample.

3.3 Catalyst preparation

The NbP powder was washed with distilled water at 70°C several times under vigorous stirring. This step is crucial to remove any residual phosphate ions due to the synthesis process. To ensure the total removal of phosphate ions, the wash water was analyzed in an INESA UV–Vis Spectrophotometer Model L9 Double Beam in an ultra-violet (UV) region. The phosphate ions absorb in the UV region at 230 nm, and the signal decrease after each wash. After the signal corresponding to phosphate disappears, the NbP is left in the oven for 24 h at 105 °C. The dry NbP was then stored in a closed flask.

3.4 Design of experiments

The experiments were designed using a face-centered composite design (FCCD). The independent variables evaluated were temperature (°C), catalyst load (g), and time (min). Table 4 shows the coded levels and variables. Times (t1, t2, t3) were selected following the criteria: T1 must be less than T3; T2 is the mean value of T1 and T3; and T1, T2, and T3 must be a multiple of 15 since aliquots were taken every 15 minutes.

Table 4 FCCD levels and variables

Variables	Abbreviation	Levels		
		-1	0	1
Temperature / °C	T / °C	140	160	180
Catalyst load / %	CL / %	1	50.5	100
Time / min	t / min	T1	T2	T3

Even though Table 4 shows three independent variables, only temperature (T), and catalyst load (CL) had defined values for FCCD. The reason for that is due to the way the pretreatment was carried out. The design consisted of a total of 19 experiments, of which 8 were factorial, 6 were faceted, and 5 were the central points (Table 5).

Table 5 FCCD with the three independent variables.

Run	Temperature / °C	Catalyst load / %	Time / min
1	140,0	1,0	t1
2	140,0	1,0	t3
3	140,0	100,0	t1
4	140,0	100,0	t3
5	180,0	1,0	t1
6	180,0	1,0	t3
7	180,0	100,0	t1
8	180,0	100,0	t3
9	140,0	50,5	t2
10	180,0	50,5	t2
11	160,0	1,0	t2
12	160,0	100,0	t2
13	160,0	50,5	t1
14	160,0	50,5	t3
15	160,0	50,5	t2
16	160,0	50,5	t2
17	160,0	50,5	t2
18	160,0	50,5	t2
19	160,0	50,5	t2

The values of time (t) were chosen by testing every combination possible following the rules early described. The minimum values are 0 min (when started) and a maximum of 135 min (when finished). For example, T1 was 0 minutes, T3 was 60 minutes, and the mean value T2 was 30 minutes.

The statistical analyses were performed by using Statistica® software (version 10.0, StatSoft, Inc). The response surfaces were made by Origin software by OriginLab version 2021.

3.5 Pretreatment

The pretreatments were performed using high-pressure and high-temperature hydrothermal reactors (Model 360L inox, Yanzheng) made of 360L stainless steel (68.7 mm × 167.5 mm), with a sampler. To the reactor was added a fixed amount of 15 g of biomass, 150 mL of ultra-pure water (10 % solid-liquid ratio), and the catalyst. The amount of catalyst for each run is shown in Table **1**3 and Table 2. The runs were made for each of SBS. After the addition of the reactants, the mixture was vigorously stirred with a glass rod, then the reactor was closed and the heating system was activated. The T was defined in Table **1**3 and Table 2. Reaching the T set, the time started to count. The stirring of the system was set to 900 rpm. Aliquots were

taken every 15 min starting at t = 0 (upon reaching the temperature) and finished at t = 135 min. When passing 135 minutes, on some occasions the fine portion of SBS could block the filter in the sample system. Additionally, taking more samples could interfere with stirring by reducing the liquid levels. After 135 minutes the reactor was immediately cooled in an ice bath until reached room temperature and atmospheric pressure.

The content of the reactor, a dark yellow liquor (liquid), and a dark brown cellulignin (solid), were separated by centrifugation. The liquors of the reactor as well as the samples were stored in a freezer at -20 °C until further analysis. The cellulignin was washed with distilled water at least 5 times or until the wash water became clean. Then the cellulignin was dried in an oven at 70 °C for 24 h. The dried cellulignin was then sealed in a vacuum and stored in the freezer at -20 °C.

3.6 Liquor analysis

The aliquots from the reaction were diluted and then filtered in a 0.22 mm nylon filter to a vial with an assistance of a 3 mL syringe. The vials were analyzed within a day or less to avoid degradation of furanic. The concentration of furanic (HMF and FF) and the carbohydrates (glucose, arabinose, and xylose) in the aliquots were determined by high performance liquid chromatography (HPLC) model Promenience (Shimadzu). The HPLC was equipped with the Bio-Rad Aminex® HPX-87H. The mobile phase was 15:85 of acetonitrile and acetic acid 0.08% m/m respectively. The flow rate was 0.8 mL/min with an oven temperature of 65 °C. The injection volume was 20 µL with a running time of 21 minutes. For carbohydrates detection was used an Evaporative Light Scattering Detector (ELSD) at 50 °C with a gain of 5. For furanic quantifications were used a Photodiode Array (PDA) in the UV region and at the wavelength of 305 nm.

The yield of the products was calculated by equation 2.

$$Y = \frac{m_p}{m_b} \qquad \textbf{Equation 2}$$

Where m_p is the mass of pentoses (arabinose and xylose) or FF in the aliquots (g), and m_b is the mass of dry biomass loaded in the reactor without the extractives.

3.7 Cellulignin analysis

The pretreated SCBs were subject to X-ray diffraction (XRD) and scanning electron microscopy (SEM).

The XRD was performed by Model D8 Discover, Bruker, with radiation Cu Kα and Ni filter. The tube potency was set at 40 kV and the current at 40 mA. The instrument was configured to acquire between 10 and 50 2-theta with an increment of 0.01 and a step time of 0.1 seconds. The samples were made in pallets of approximately 1.3 cm. The relative crystallinity index (CrI) was calculated following equation 3, an empirical method proposed by Segal et al. (1959) (SEGAL et al., 2016).

$$CrI = \frac{\left(I_{002} - I_{am}\right)}{I_{002}} \times 100 \qquad \textbf{Equation 3}$$

where I_{002} is the maximum intensity (in arbitrary units) of the 002 lattice diffraction and I_{am} is the intensity of diffraction in the same unit at $2\theta = 18°$.

The surface images were taken under an SEM JEOL JSM 6010LA microscope. Samples were fixed on stubs by double-sided carbon tape and then its surface was covered with gold in a Quorum Q150R S Sputter coater instrument. Secondary electron imaging at 10 mm of work distance and 10 kV of potency was used in the analysis. Energy-Dispersive X-ray spectroscopy (EDS) was performed with the same instrument which obtained SEM images. The elements carbon, oxygen, niobium, phosphorus, and silicon were chosen to create a chemical mapping.

4. RESULTS

4.1 Characterizations

The granulometry distribution of the three SBS is shown in Figure 13. The granulometry was analyzed after the washing, grinding, and drying process. The result is shown in the percentage of each fraction retained in the sieves corresponding to the respective biomass.

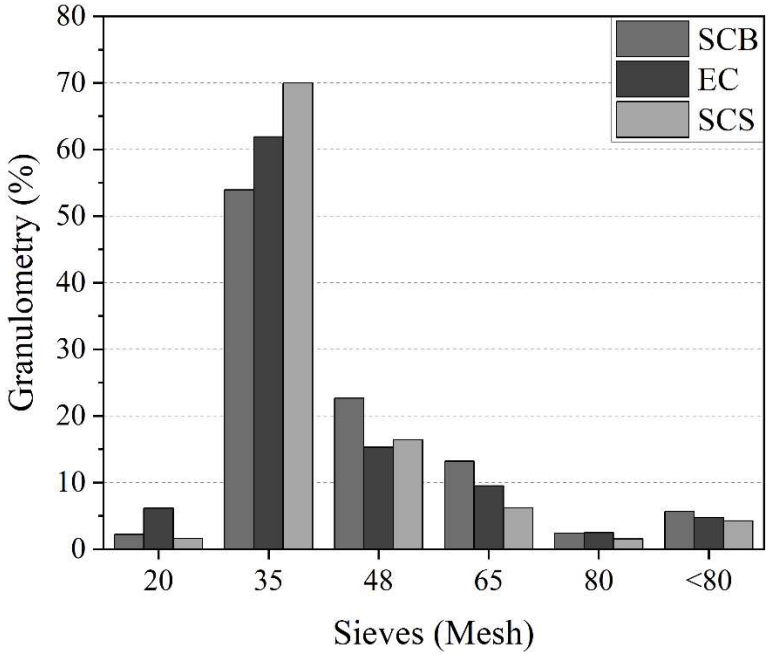

Figure 13 Granulometry distribution of SBS.

Figure 13 shows the same pattern distribution of all SBS. For all SBS a greater fraction was found in the sieves of 35 and 48 mesh representing approximately 72-86 % of the ground SBS. The SCB has shown the least biomass retained in a 35 mesh, showing overall thinner particles if compared to the others. The SCS has presented the opposite with a large portion of the particle retained in the 35 mesh and the EC presenting the middle term. This could be affected by several factors such as the previous grind (as received), the type of the SBS, or moisture content (OYEDEJI et al., 2020; PROBST et al., 2013). In this case, the type of SBS could be the biggest influencer since the EC, which contained a mixture of juice, straw and bagasse, has achieved the middle term between SCB and SCS.

The values of moisture content are displayed in Figure 14. The analysis was made in triplicate.

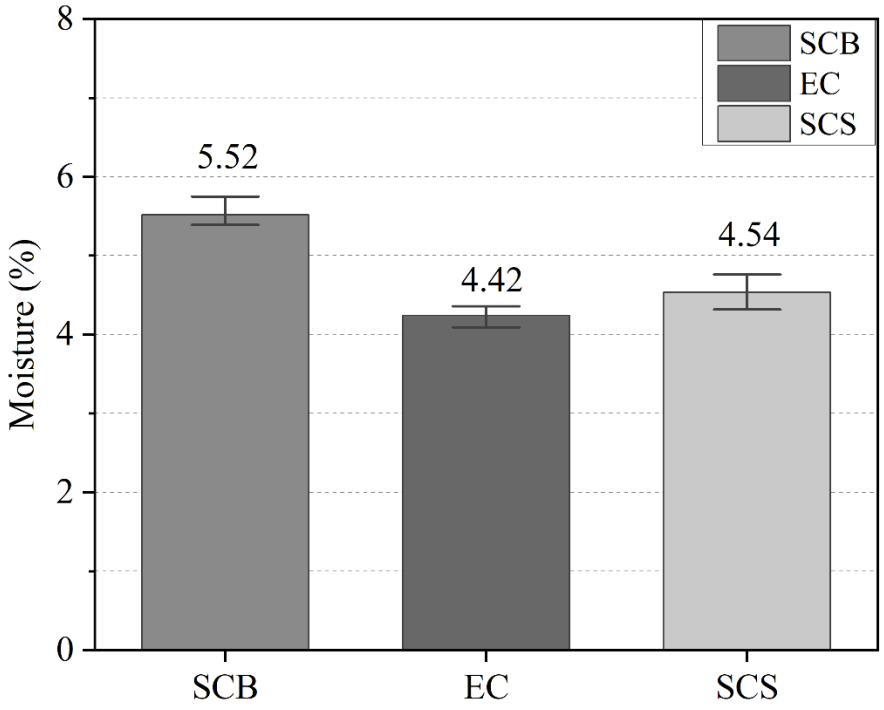

Figure 14. The moisture content of sugarcane bagasse (SCB), sugarcane straw (SCS), and energy cane (EC).

As shown in Figure 14, all three SBS presented relatively low levels of moisture with the mean value range going 4.42 to 5.52. Low moisture content is desirable in different aspects. A moisture content below 10 % is required for the biomass to be suitable for carbohydrate analysis as specified in the National Renewable Energy Laboratory (NREL) procedure. According to Sluiter et al., 2008, moisture above 10 % will interfere with appropriate acid concentrations (SLUITER et al., 2008). A high moisture level also increases water activity leading to an increase in microbial levels and therefore degradation and mass loss. To avoid microbial activity is recommended moisture below 15 % allows safe long-term storage of biomass (RENTIZELAS, 2016). The method of drying in a recirculation oven shows highly effective since the moisture content of SBS has present below 10 or 15 %.

The ashes content is shown in Table 6. The higher ashes content has been found in SCS (5.80 %) and the lower content in SCB (2.14). The EC has presented, as in granulometry, the middle term, this was expected since was a mixture of straw and bagasse.

Table 6 Ashes content for all SBS.

Experiment	Ashes (%)		
	SCB	**EC**	**SCS**
1	2.05	2.94	5.62
2	2.22	2.86	6.07
3	2.15	2.99	5.72
Average	2.14	2.92	5.80
SD	0.09	0.07	0.24

SD: Standard Deviation

The results presented in Table 6 agreed with the ones found in the literature. The ashes content of SCS can vary from 4.05 to 9.75 while SCB varies from 2.30 to 3.91 (ÁVILA; FORTE; GOLDBECK, 2018; CARVALHO et al., 2015; PALMA et al., 2021). Certain amounts of ashes are usually associated with contamination of inorganics from the soil, along with mechanical equipment such as titanium and iron (SZCZERBOWSKI et al., 2014). The higher amounts of ashes present in SCS could be associated with the contamination of soil and dirt during the harvest.

The chemical composition of SBS is a crucial step to calculate the yield of the interest compounds (FF, xylose, and arabinose). The results of carbohydrates, lignin, and extractives are presented in Table 7.

Table 7 Chemical composition of raw SBS.

Biomasses	Extract. (%)	Lignina			Carbohydrates (%)[4]				
		Sol[1] (%)	Ins[2] (%)	Total[3] (%)	Ara	Gal	Glu	Xyl	Man
EC	11.14	1.52	16.85	18.37	2.1	0.6	40.0	17.9	0.5
	11.20	1.63	16.79	18.41	2.1	0.6	40.2	17.9	0.5
Average	**11.17**	**1.57**	**16.82**	**18.39**	**2.1**	**0.6**	**40.1**	**17.9**	**0.5**
Bagasse	4.69	1.54	17.37	18.91	2.5	0.7	43.4	21.3	0.0
	5.06	1.47	17.76	19.23	2.5	0.7	43.1	21.1	0.0
Average	**4.88**	**1.51**	**17.56**	**19.07**	**2.5**	**0.7**	**43.2**	**21.2**	**0.0**
Straw	9.50	1.85	17.27	19.12	3.0	0.8	39.1	19.5	0.0
	9.65	1.91	17.21	19.12	3.0	0.8	39.7	19.6	0.0
Average	**9.58**	**1.88**	**17.24**	**19.12**	**3.0**	**0.8**	**39.4**	**19.6**	**0.0**

[1]Soluble lignin, [2]Insoluble lignin, [3]Total lignin, [4]Carbohydrates: Arabinose, Galactose, Glucose, Xylose, and Mannose

The SCB showed the highest relative glucose and pentoses among SBS, 43.2 and 24.4 respectively. Rocha et al., 2014 showed similar results for the SCB characterization with an

average of 42.2% glucose and 27.6% pentoses (ROCHA et al., 2015). The composition of SCS also presented similar results to studies of Saad et al., 2008 with the same values of glucose at 39.4% and 26.2% of pentoses (23.4% of this work)(SAAD et al., 2008). Qiu et al., 2012 found a chemical composition of EC similar to this work, their study presented 40.87 % glucose and 22.35 % pentoses (this work, 40.1%, and 20.6%, respectively) composition.

A high amount of extractives were found in SCS and EC. This could be visible during the washing process with water and ethanol, presenting a darker wash liquid if compared to SCB. The removal partially or totally of extractives avoided matrix effects in HPLC analysis. This demonstrated the importance of the washing step during the study.

4.2 Pretreatment

The results presented in Figure 15 show the difference that the catalyst could do in the pretreatment. The condition chosen was the SCB at 170 °C and the catalyst at 100 % (1:1 biomass catalyst ratio).

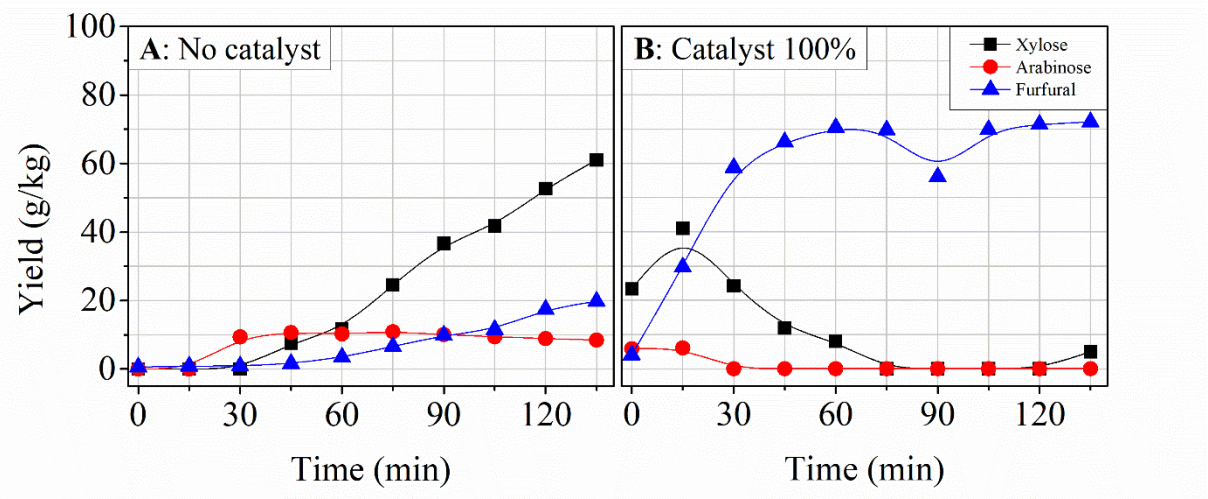

Figure 15. SCB pretreatment comparison between the absence (A) and the presence (B) of NbP as the catalyst. Experimental conditions: Temperature of 170°C, and for the presence of the catalyst (NbP) was choose a 100 % load.

For the carbohydrates, the arabinose was released earlier than xylose, this can be seen more clearly in Figure 15A at 30 minutes. The early release of arabinose could be because of the easy access to this carbohydrate in the structure. Carvalho et al. (2017) have proposed an empirical structure of SCB and SCS hemicellulose (MORAIS DE CARVALHO et al., 2017). The structure consists mainly of xylose units bonded in a chain with ramifications of arabinose, glucose, and acetyl groups. Thus, the release of the ramification groups seems to occur first and then the main chain.

As Figure 15 shows, the catalyst had a great impact on the pretreatment not only in the release of the hemicellulose but in the conversion of the carbohydrates in FF. At t = 0 minutes, the pretreatment without catalyst had shown no evidence of the solubilization of hemicellulose. However, by this time the pretreatment with the catalyst showed yields of xylose and arabinoses implying that the hemicellulose had already started to break before the first aliquot was taken. In Figure 15B, a conversion is seen since the xylose and arabinose yields reduce the FF yield increase. The maximum xylose yield was found at 15 minutes, after this point, the release of xylose is overcome by the conversion in FF.

The NbP has demonstrated great activity in covert xylose and arabinose in FF. In the pretreatment without the catalyst (Figure 15A), the conversion of xylose to FF seems to occur in a lower ratio than the release of xylose. This resulted in a higher yield of xylose than FF. In opposition, the pretreatment with catalyst (Figure 15B) at 15 minutes, xylose had reached the maximum and at 75 minutes, practically all pentoses had converted in FF. The NbP had demonstrated accelerated solubilization of hemicellulose and conversion of pentoses reactions.

Figure 16,Figure **17**, and Figure **18** shows the pretreatment experiments carried out following the conditions shown in Table 5. For comparison purposes, all graphs for each SBS will be presented with the same scale.

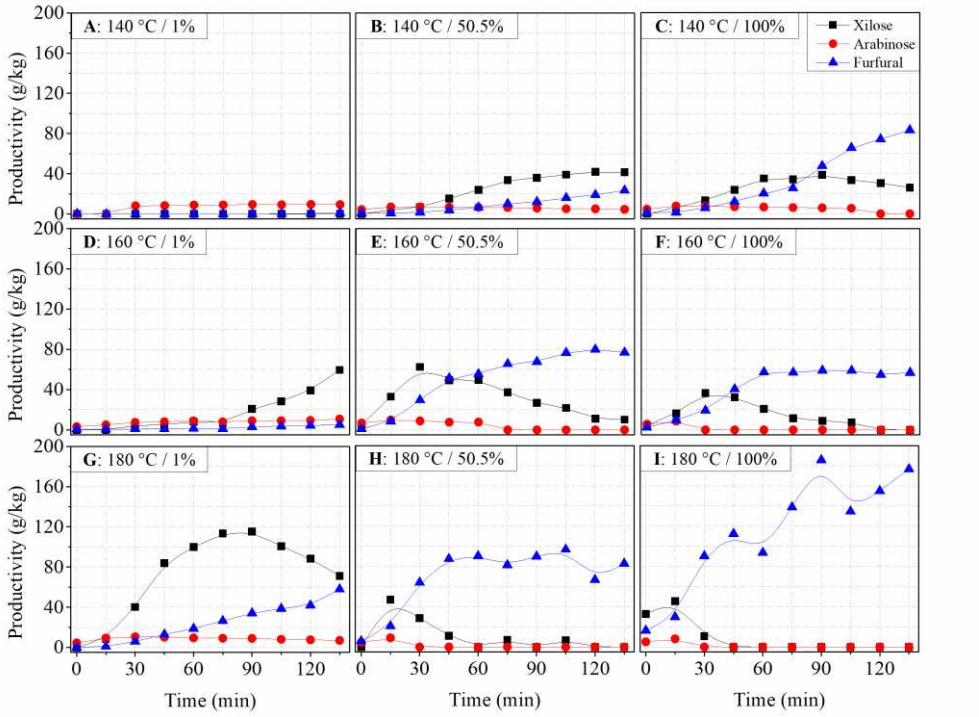

Figure 16. Pretreatments of SCB according to the FCCD. In the horizontal orientation, it shows pretreatments at the same temperature, and in the vertical orientation the same catalyst load.

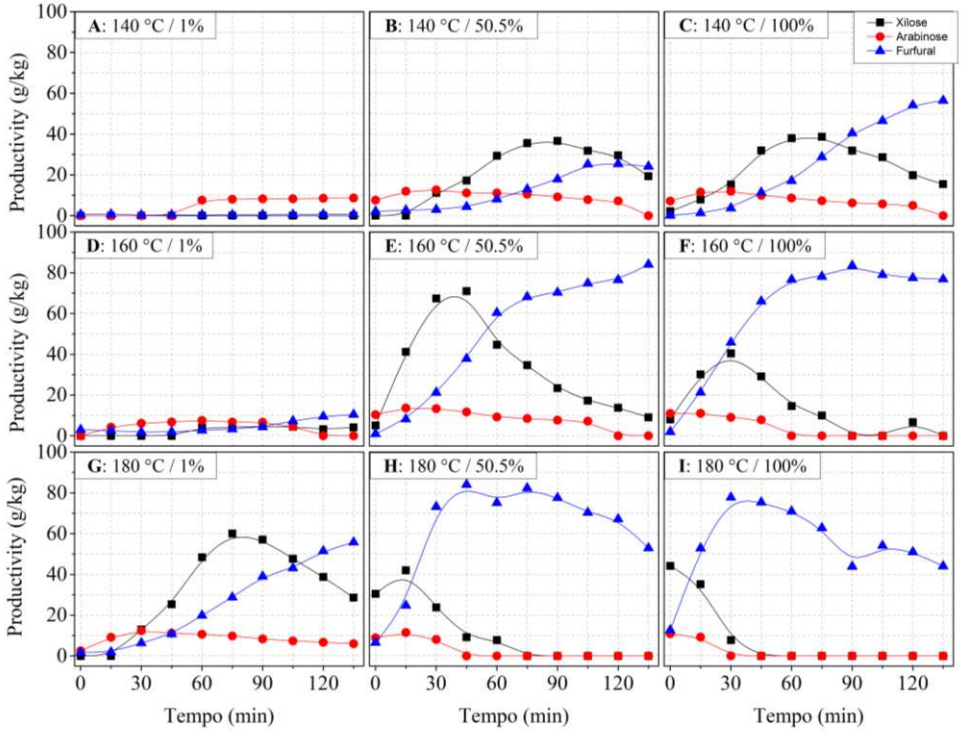

Figure 17. Pretreatments of SCS according to the FCCD. In the horizontal orientation, it shows pretreatments at the same temperature, and in the vertical orientation the same catalyst load.

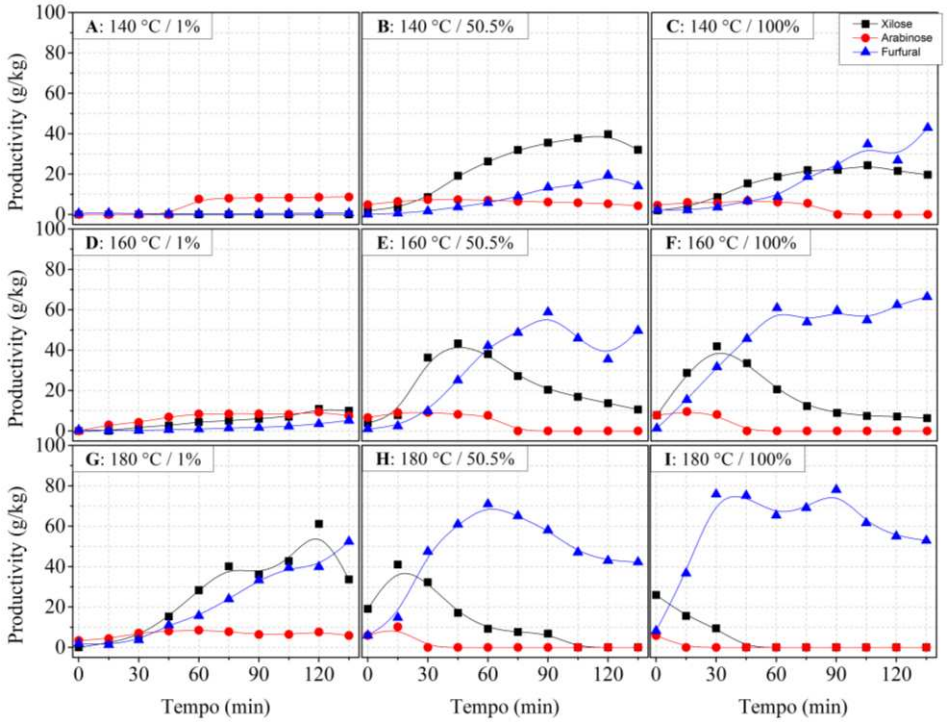

Figure 18 Pretreatments of EC according to the FCCD. In the horizontal orientation, it shows pretreatments at the same temperature, and in the vertical orientation the same catalyst load.

It was observed in Figure 16 that with low CL (A, D, G) an increase in the T provided more hemicellulose solubilization. In this case, achieved a higher yield of xylose in G around 90 minutes (115 g/kg) with a relatively low yield of FF (34 g/kg). At the horizontal orientation (same T), the increase in CL provided more hemicellulose solubilization as shown in Figure 16 (e.g. D, E, F). However, the increase in CL also increases the conversion of xylose in FF. The odd behavior found in I could be due to the polymerization and condensation of FF favored by the presence of the catalyst, as shown by Wang et al., 2018 (WANG et al., 2018).

The SCB and SCS pretreatments results have similar patterns. The maximum xylose yield for both was found in Figure 15E at 45 minutes (71 g/kg). In high-severity conditions and high CL (Figure 17H and I), high FF yields were achieved but decreased over t. This could be by the formation of hydrochar due to the condensation and polymerization of FF(WANG et al., 2018). Despite similar patterns, SCS overall yields had demonstrated considerably lower than SCB yields. A reason for this phenomenon could be the number of acetyl groups in the hemicellulose fraction of the SCS. During the hemicellulose solubilization, ester bonds are hydrolyzed forming acetic acid, which could catalyze the degradation of hemicellulose (RUIZ; THOMSEN; TRAJANO, 2017). Therefore, the more acetyl groups hydrolyzed more acetic acid in the medium. The study of Carvalho et al., 2017 has demonstrated that SCB has more ramifications containing acetyl groups than SCS hemicellulose.

The results for EC are presented in Figure 18. The higher xylose yield was found in Fig.16G at 120 minutes (61 g/kg). The conditions with high T and high CL also demonstrated a decrease in FF yield, probably by the formation of hydrochar and consumption of FF(WANG et al., 2018).

The condensation and polymerization of the FF are responsible for the formation of hydrochar, a carbonaceous black material. The hydrochar formation depends heavily on the T, in which high T decrease H/C and O/C ratios (WANG et al., 2018). Results from Figure 19 shows the cellulign after the pretreatments presented in Figure 16, Figure **17**, and Figure **18**. The most noticeable characteristic of pretreated SBS is the color change. There are two main reasons for this change, first is the formation of hydrochar increasing with the severity of pretreatment. Another aspect is the formation of droplets of lignin dissolved and recondensed during the pretreatment. These droplets give the cellulign a darker color as shown in Nitsos et al., 2013. The deposition of lignin on the surface is not desirable since forms a physical barrier to the enzymatic process (LI et al., 2014).

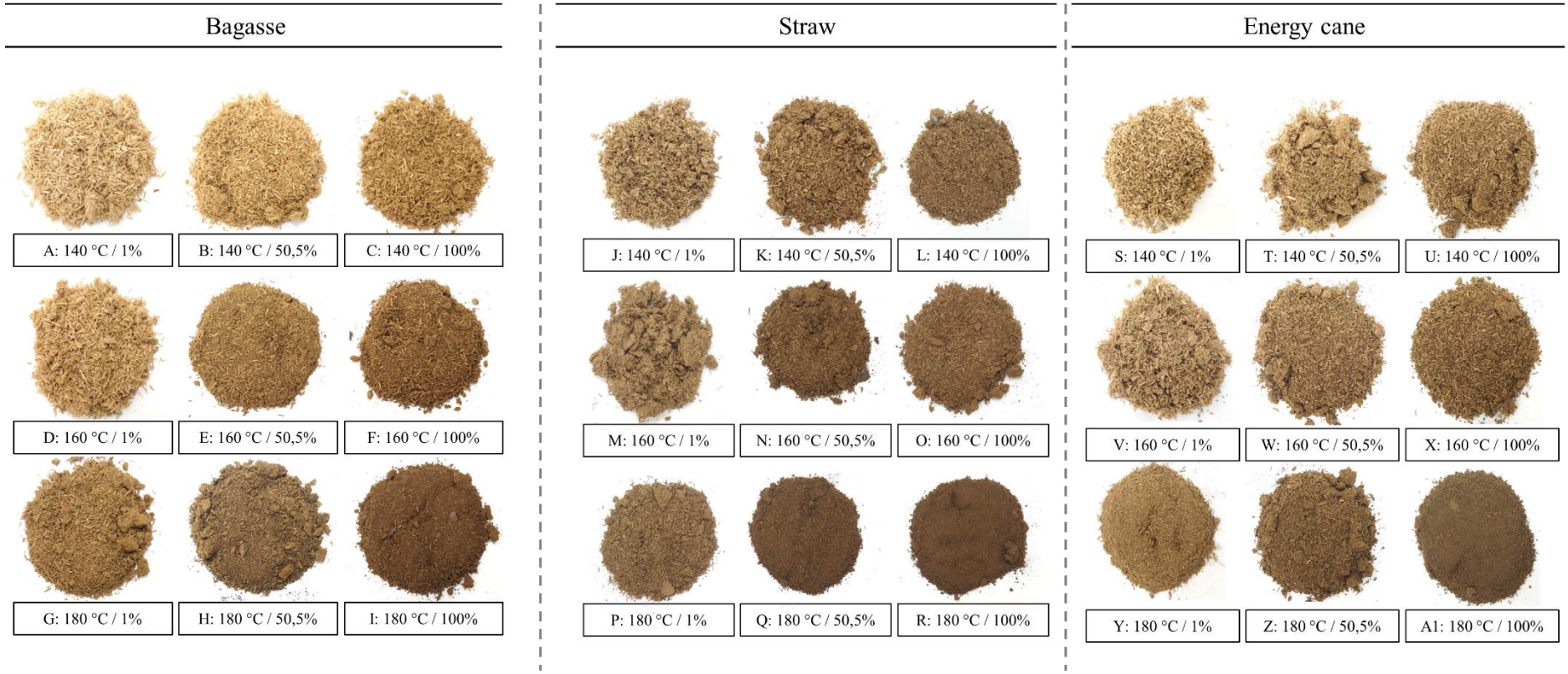

Figure 19. Images of SCB (A to I), SCS (J to R), and EC (S to A1) cellulign after the pretreatment following the respective conditions.

The other aspect of the cellulign in Figure 19 is the granulometry for each pretreatment. In Figure 19 A, the color and granulometry are visually very similar to the SCB which started. However, when increasing the T and the CL the color becomes darker and the granulometry finer.

The images shown in Figure 17. (J to R) are of SCS cellulignin after the pretreatment. Similar results to SCB images (Figure 19 A to I) were found, the main difference is based that SCS was naturally darker than SCB. However, the condition of higher T and high CL had similar color and granulometry.

The start coloration of EC (Figure 19 S) is an intermediate between SCB and SCS. This is because EC is a mixture of straw and bagasse. However, in conditions with higher T and higher CL, the cellulignin behavior as the others became darker and finer.

4.3 Statistical analysis

The independent variable t was defined as the lower level of 0 minutes and the upper level of 60 minutes for analysis of SCB and EC. This interval was chosen because is when started the sampling and higher than 60 some degradation reactions had taken place. For SCS analysis t was defined as the lower level 0 and the upper level 30 minutes. Within this interval of t, the xylose and FF had almost reached the maximum values, choosing greater times would be considered side reactions from FF

The responses used in the model's creation were pentoses and FF. Table 8 shows the decoded variables as the respective responses for SBS. For all statistical analyses pure error was used since were made replicates in the central point. The standard error coefficient that appears in Table 8 measures how precisely the model estimates the coefficient's unknown value. Ideally, this error should be zero or much smaller than the coefficient value.

Table 8. Independent variables used in FCCD and respective responses of pentoses and FF for SBS.

Bagasse					Straw			Energy cane		
Independent variables		Independent variable	Responses		Independent variable	Responses		Independent variable	Responses	
T (°C)	CL (%)	t (min)	Pent[a] (g/kg)	FF[b] (g/kg)	t (min)	Pent[a] (g/kg)	FF[b] (g/kg)	t (min)	Pent[a] (g/kg)	FF[b] (g/kg)
140	1	0	0.00	0.22	0	0.00	0.55	0	0.00	0.64
180	1	0	4.54	0.00	0	2.50	1.69	0	3.42	1.92
140	100	0	4.60	1.02	0	9.33	0.13	0	6.60	2.34
180	100	0	37.98	16.35	0	55.04	12.65	0	31.82	8.18
140	1	60	8.83	0.00	30	0.00	0.29	60	5.23	0.18
180	1	60	109.43	18.77	30	25.39	6.32	60	36.85	15.65
140	100	60	41.93	20.49	30	27.22	3.70	60	24.84	8.79
180	100	60	0.00	93.67	30	7.76	77.75	60	0.00	65.34
140	50.5	30	13.79	1.60	15	11.99	2.68	30	15.92	1.70
180	50.5	30	28.55	63.99	15	53.55	24.76	30	32.20	47.49
160	1	30	11.79	0.88	15	4.24	2.57	30	6.11	0.24
160	100	30	36.61	19.26	15	41.17	21.30	30	50.10	31.66
160	50.5	0	11.95	0.97	0	15.45	0.97	0	10.59	0.99
160	50.5	60	57.29	55.48	30	80.77	21.25	60	45.76	42.12
160	50.5	30	71.37	29.59	15	54.86	8.15	30	45.51	9.80
160	50.5	30	64.61	16.19	15	52.49	9.50	30	57.71	15.45
160	50.5	30	62.17	12.99	15	40.49	8.66	30	44.64	10.91
160	50.5	30	46.58	10.88	15	27.48	5.70	30	50.53	11.46
160	50.5	30	43.53	11.24	15	28.34	0.98	30	45.69	21.94

Pent[a] = Pentoses and FF[b] = Furfural.

The statistical model for pentoses and FF from SCB can be seen in Table 9.

For pentoses, the variables that appear significant were T and t linear. The variable CL has not present statistical significance. However, the interaction of time and CL shows significance. The lack of fit also presents statistical significance meaning that the model fails to adequately describe the relationship between the experimental data and the response. The reason for that could be the complexity of the hemicellulose and the several reactions occurring at the same time. The xylan goes through the process of hydrolysis to xylooligomers, then xylooligomers are broken into xylose (YU et al., 2020). Other reactions as the conversion of xylose to xylulose (Figure 10) could also interfere since the catalyst was added.

The results presented in Table 9 for FF, show that the most statistically significant variables were linear, followed by the interaction of these three. These linear variables were positive meaning that in the interval studied all three variables increase the response by shifting from the lower level to the higher level studied. The lack of fit was not statistically significant that is the model adequately describes the relationship between the experimental data and the response. Thus, the corresponding response surface could be applied.

The better condition to produce FF with SCB was using 100 % of CL, a T of 180 °C, and a t of 60 minutes. This condition produced an FF yield of approximately 95 g/kg.

The statistical models for pentoses and FF from SCS can be seen in Table 10.

The lack of fit presented by the pentoses model had not been significant. However, the model showed that no variable nor interaction was significant either. An explanation could be in the pure error of the analysis, which is high. This demonstrated that the reproducibility of pentoses was not great. Therefore, no response surface was applied since no variables were statistically significant.

The FF model showed statistical significance for all three linear variables and the interactions. For better adjustment of the model, the quadratic variables were removed since they were not significant. All the variables showed positive coefficients, which means that the response increased as the variables passed from the lower level to the higher level. The lack of fit was not statistically significant, that is the model adequately describes the relationship between the experimental data and the response. Thus, the corresponding response surface could be applied.

The better condition to produce FF was using 100 % of CL, a T of 180 °C, and a t of 30 minutes. This condition produced an FF yield of 77,75 g/kg.

Table 9. Coefficients and lack of fit using pentoses and FF response for SCB.

	Bagasse					
	Pentoses			Furfural		
	Coefficient	Error†	p^{**}	Coefficient	Error	p^{**}
Intercept	*47.5*	*4.40*	*4.2×10^{-4}*	*19.5*	*2.85*	*2.41×10^{-3}*
(1)T (L)	*11.1*	*3.80*	*4.3×10^{-2}*	*16.9*	*2.46*	*2.34×10^{-3}*
T (Q)	-13.7	7.28	0.13	9.22	4.71	0.120
(2)CL(L)	-1.34	3.80	0.74	*13.1*	*2.46*	*6.02×10^{-3}*
CL(Q)	-10.7	7.28	0.21	*-13.5*	*4.71*	*4.56×10^{-2}*
(3)t (L)	*15.8*	*3.80*	*0.014*	*17.0*	*2.46*	*2.32×10^{-3}*
t (Q)	-0.309	7.28	0.97	4.65	4.71	0.380
1L by 2L	*-14.2*	*4.25*	*0.029*	*8.75*	*2.75*	*3.36×10^{-2}*
1L by 3L	2.59	4.25	0.57	*9.61*	*2.75*	*2.51×10^{-2}*
2L by 3L	*-14.2*	*4.25*	*0.028*	*9.78*	*2.75*	*2.37×10^{-2}*
Lack of Fit			*3.2×10^{-2}*			0.109
R sqr	0.59			0.88		

Variables in italic are significant at α = 0.05. †Error pure for coefficients

***p-value.*

Table 10. Coefficients and lack of fit using pentoses and FF response for SCS.

	Straw					
	Pentoses			Furfural		
	Coefficient	Error†	p^{**}	Coefficient	Error	p^{**}
Intercept	*41.8*	*4.73*	*9.07×10^{-4}*	*11.0*	*0.79*	*1.53×10^{-4}*
(1)T (L)	9.57	4.08	7.91×10^{-2}	-	-	-
T (Q)	-10.3	7.81	0.263	*11.6*	*1.09*	*4.43×10^{-4}*
(2)CL(L)	10.8	4.08	5.67×10^{-2}	-	-	-
CL(Q)	-20.3	7.81	5.99×10^{-2}	*10.4*	*1.09*	*6.69×10^{-4}*
(3)t (L)	5.88	4.08	0.222	-	-	-
t (Q)	5.07	7.81	0.551	*9.33*	*1.09*	*1.02×10^{-3}*
1L by 2L	-0.210	4.57	0.974	*9.93*	*1.22*	*1.23×10^{-3}*
1L by 3L	-5.29	4.57	0.311	*8.30*	*1.22*	*2.42×10^{-3}*
2L by 3L	-6.54	4.57	0.232	*8.04*	*1.22*	*2.73×10^{-3}*
Lack of Fit			0.114			0.106
R sqr	0.60			0.90		

Variables in italic are significant at α = 0.05. †Error pure for coefficients

***p-value.*

Table 11. Coefficients and lack of fit using pentoses and FF response for EC.

	Energy cane					
	Pentoses			Furfural		
	Coefficient	Error†	p^{**}	Coefficient	Error	p^{**}
Intercept	*43.7*	*2.01*	*2.63×10^{-5}*	*15.6*	*1.14*	*1.64×10^{-4}*
(1)T (L)	*5.17*	*1.73*	*4.06×10^{-2}*	-	-	-
T (Q)	*-13.3*	*3.32*	*1.60×10^{-2}*	*12.5*	*1.57*	*1.36×10^{-3}*
(2)CL(L)	*6.18*	*1.73*	*2.35×10^{-2}*	-	-	-
CL(Q)	*-9.25*	*3.32*	*4.94×10^{-2}*	*9.77*	*1.57*	*3.41×10^{-3}*
(3)t (L)	*6.03*	*1.73*	*2.54×10^{-2}*	-	-	-
t (Q)	-9.18	3.32	5.04×10^{-2}	*11.8*	*1.57*	*1.68×10^{-3}*
1L by 2L	-4.33	1.94	8.91×10^{-2}	*5.71*	*1.76*	*3.14×10^{-2}*
1L by 3L	-2.73	1.94	0.232	*8.11*	*1.76*	*9.89×10^{-3}*
2L by 3L	*-6.53*	*1.94*	*2.81×10^{-2}*	*6.29*	*1.76*	*2.31×10^{-2}*
Lack of Fit			*1.17×10^{-2}*			6.46×10^{-2}
R sqr	0.69			0.82		

Variables in italic are significant at α = 0.05. †Error pure for coefficients

***p-value.*

The statistical models for pentoses and FF from EC are presented in Table 11.

The variable CL and lack of fit for pentoses showed statistical significance. The reasons for that could be the same as those explained for SCB. Therefore, no response surface was applied for pentoses.

For FF, the quadratic variables were removed since neither showed statistical significance. These coefficients were also positive, meaning that the response increased as the variables increased in level. The lack of fit was not statistically significant; the model adequately describes the relationship between the experimental data and the response. Thus, the corresponding response surface was applied.

The FF yields responses surfaces are shown in Figure 20 for SBS. All SBS present similar patterns in the response surface. Overall, the FF yield increases as the levels increase; that is, the FF production is augmented by rising temperature, time, and catalyst load. Among the surfaces, SCB (A and B) had shown curvature, unlike SCS and EC (C to F). This result is due to the significant quadratic variable (Table 8). To obtain the surface, t and CL were fixed. t was fixed at 60 minutes for SCB and EC (A and E) and 30 minutes for SCS (C). The CL was fixed at 100 % for all biomasses (B, D, and F).

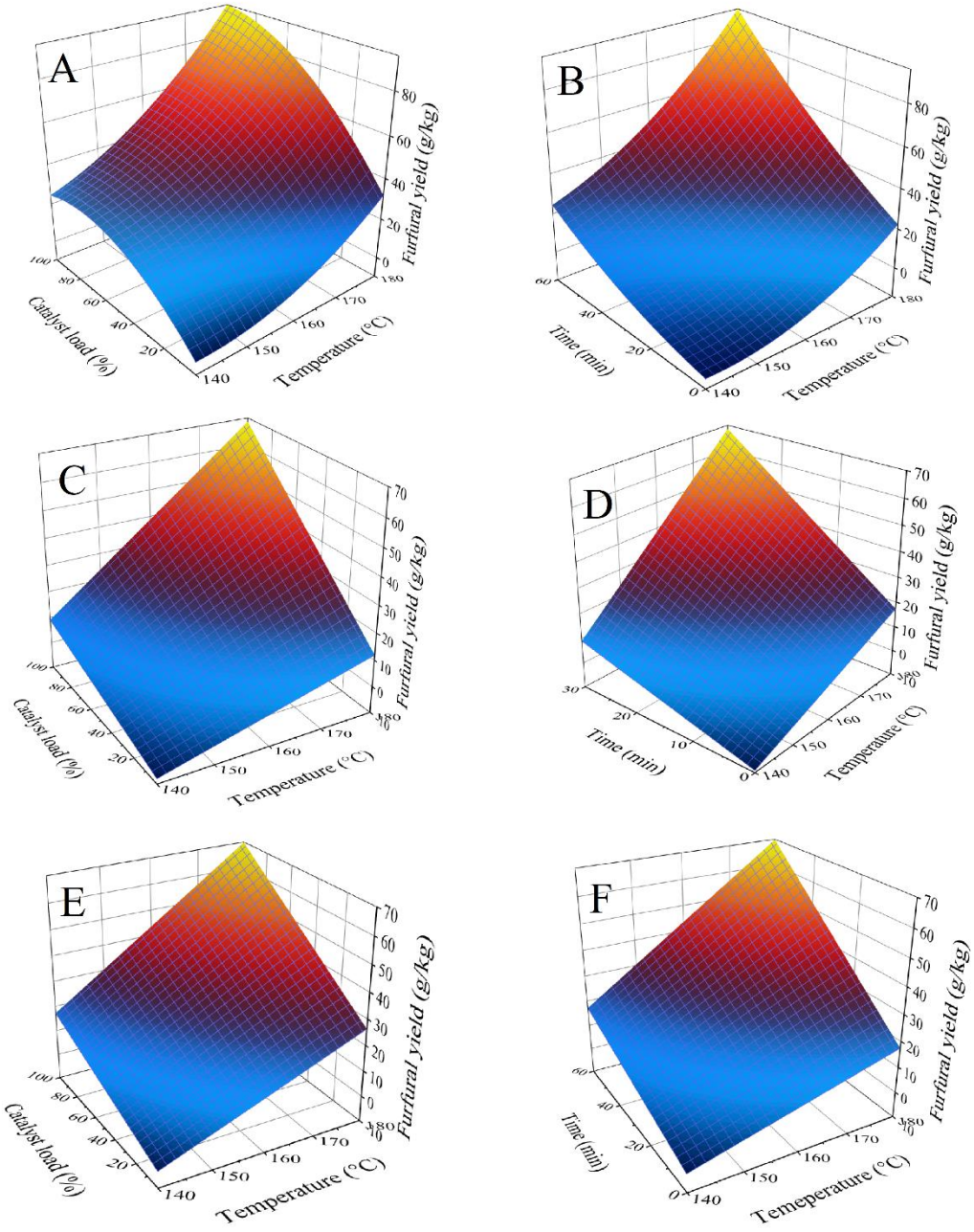

Figure 20. Responses surfaces of FF yield as the function of temperature and time and the function of temperature and the catalyst load for SCB (A and B), SCS (C and D), and EC (E and F).

Table 12. Maximum yields of pentoses and FF for SBS

	Pentoses g/kg				Furfural g/kg			
	T (°C)	t (min)	CL (%)	Yield (g/kg)	T (°C)	t (min)	CL (%)	Yield (g/kg)
SCB	180	90	1	124.1	180	60	100	95.0
SCS	160	45	50.5	82.0	180	30	100	68.6
EC	180	120	1	68.7	180	60	100	69.8

The maximum SBS yields of pentoses and FF are present in Table 11. The maximum pentoses yield was obtained by experimental data since the models fail to adjust. For FF maximum yield, the values were obtained by the prediction of the model within the levels studied.

4.4 SCB cellulignin characterization

4.4.1 x-ray diffraction

The x-ray diffractions of SCB pallets were made to understand the crystalline structure of the biomass. The cellulose structure presents two peaks in an x-ray diffractogram. The first is less intense at 2-theta of 15° and the second is more intense at 2-theta of 22°. For CrI analysis, the valley between these two peaks at approximately 2-theta of 18° and the more intense peak are used to estimate the relative crystallinity.

Figure **21** shows the x-ray diffractogram of SCB raw, SCB pretreat, and pure cellulose. The cellulose appeared as the most crystalline of the three followed by the pretreated SCB and the raw SCB.

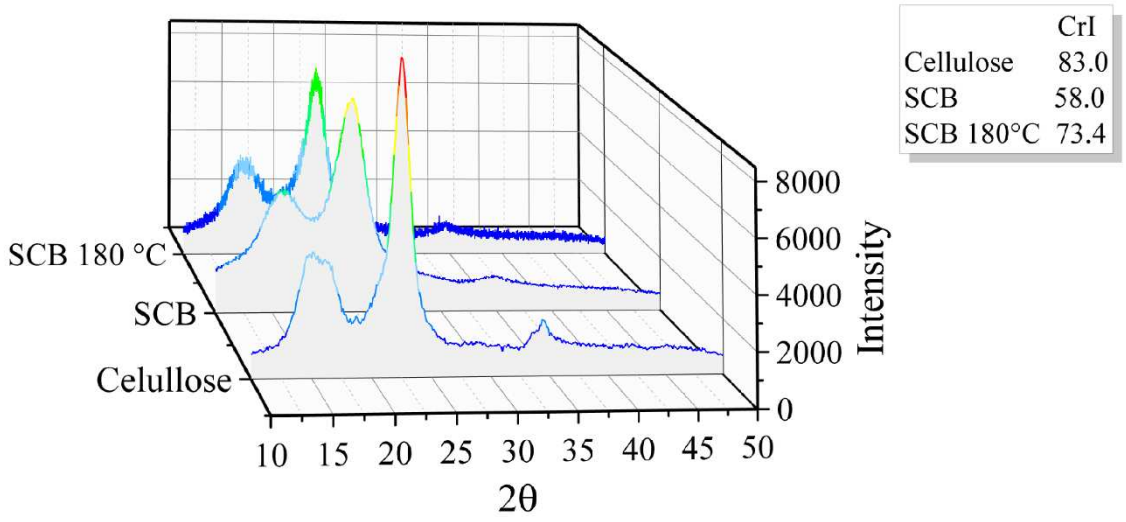

Figure 21. x-ray diffractogram of raw cellulose (front), raw sugarcane (middle), and pretreat SCB at 180 °C with 1 % catalyst load (back).

After the pretreatments, the CrI tends to increase primarily due to the removal of the amorphous components of the biomass (hemicellulose and lignin) leaving the crystalline cellulose (KIM et al., 2003).

Figure 21 shows the x-ray diffractogram of SCB after three conditions of pretreatment. These conditions were with the same CL of 1% but at different T. The CrI values indicate that in high T the removal of the amorphous region was greater. These results corroborate with Figure 16 (A, D, and G), as showed that pentoses were released of the SCB.

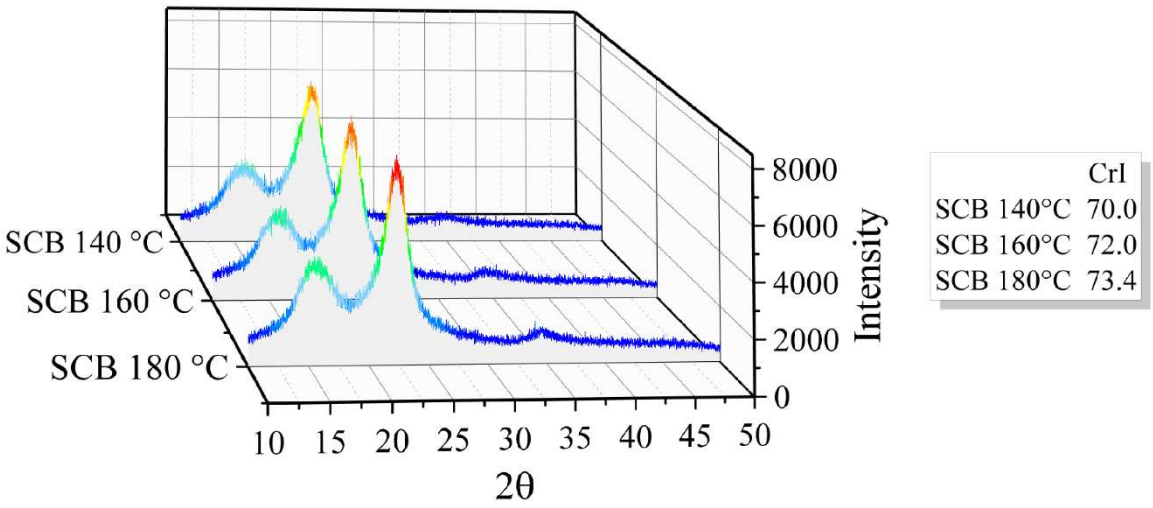

Figure 22. x-ray diffractions from different pretreatment conditions for SCB. The experimental conditions were 1% of NbP and temperatures of 140 °C (back), 160 °C (middle), and 180 °C (front).

4.4.2 Screening electronic microscopy and Energy-Dispersive x-ray Spectroscopy

The morphological study of SCB was studied by SEM images as the EDS analysis. Figure 23 shows the SEM images of SCB before and after the pretreatment. The conditions of the pretreatment were 170 °C and 50 % CL. Before the pretreatment, it is possible to observe a smooth surface (Figure 23 a and b). The flake in Figure 23a is probably due to the milling process. This smooth surface from the raw SCB is also seen in the study of Nitsos et al. (2013), which compared the morphological structure in different pretreatment (NITSOS; MATIS; TRIANTAFYLLIDIS, 2013).

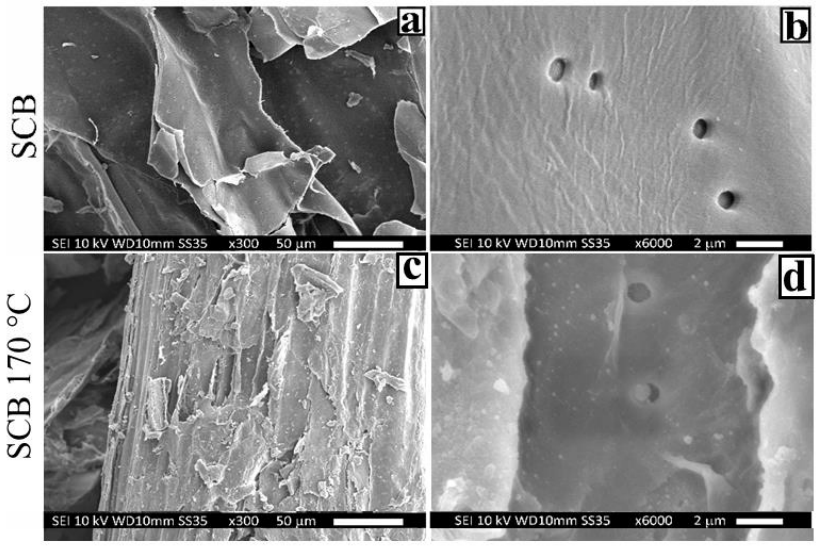

Figure 23. SEM images of SCB before (a and b) and after pretreatment (c and d). Pretreatment conditions: 170 °C and 50 % catalyst load.

After the pretreatment, it was seen that the surface of SCB is altered (Figure 23c). The lignin droplets were dissolved and recondensed on the surface of the SCB (Figure 23c). These droplets give the SCB a darker brown color if compared to the raw biomass as shown in Figure 19. Thus, the pretreatment seems to improve the superficial area of the biomass by breaking down the microstructure and creating porous. The higher surface area would enhance the contact of enzymes and the SCB improving the enzymatic process (NITSOS; MATIS; TRIANTAFYLLIDIS, 2013).

The EDS images presented in Figure 24 provided a chemical map of the SCB surface. Figure 24A is the original image with 1000 x magnified. The carbon and oxygen are shown in Figure 24B and Figure 24C), and as expected it was fairly distributed since the major component of SCB are carbohydrates.

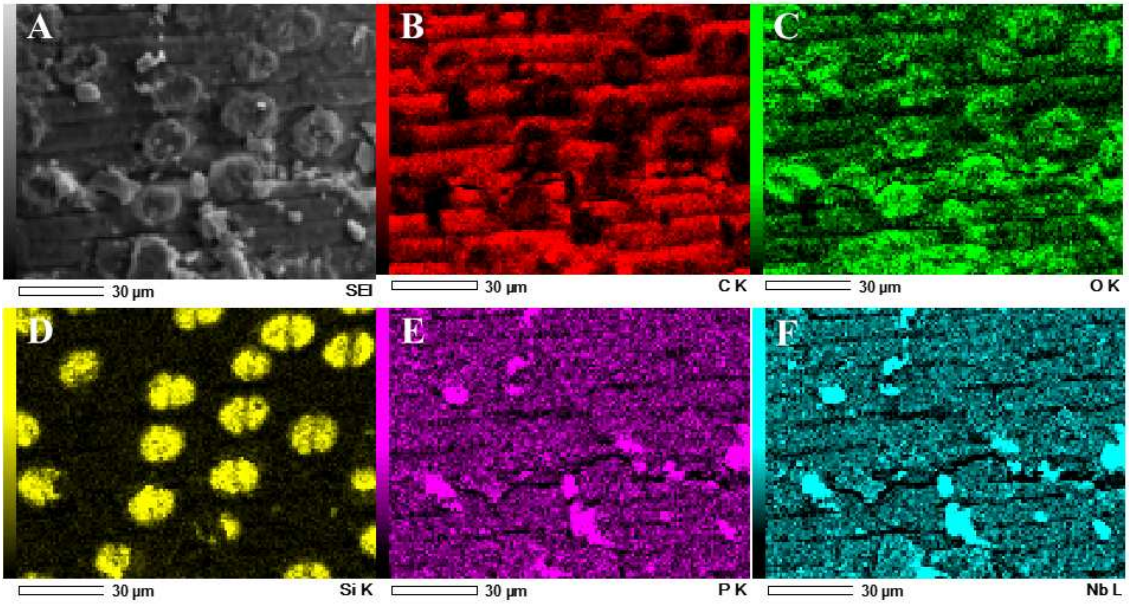

Figure 24. EDS images of SCB, the original image (A), and the chemical map of carbon (B), oxygen (C), silicon (D), phosphate (E), and niobium (F).

The yellow dumbbell-shaped spot in Figure 24D is due to the formation of silica bodies. The silica bodies are composed of silicon and distributed in the tissue as well localized in phytoliths (NEGRÃO et al., 2021). Figure 24E and F shows the distribution of NbP over the SCB surfaced.

5. CONCLUSION

The niobium phosphate demonstrated that is an effective catalyst in the pretreatment of sugarcane biomasses. By using this catalyst, it is avoided the use of a homogeneous catalyst such as mineral acids that generate waste, provokes corrosion, and is hard to recover.

The yield of FF and xylose has shown similar patterns for SCB, SCS, and EC. However, the maximum yield of xylose differs in each case. The FF was modeled to obtain the maximum yield and a surface of response was applied for each biomass. The linear variables showed to be statistically significant in all cases. The highest yield predicted was in the upper levels of temperature and catalyst load within the time selected. The yields of FF decreased at higher times, showing the formation of humins and hydrochar changing the color of the biomasses.

Thus, this work showed a variety of pretreatment for three biomasses in different conditions using um solid catalyst. Therefore, making it is easier to achieve the goal whether it is to produce FF or release xylose from hemicellulose.

6. REFERENCES

AKIA, M. et al. A review on conversion of biomass to biofuel by nanocatalysts. **Biofuel Research Journal**, v. 1, n. 1, p. 16–25, March 1. 2014.

ALALWAN, H. A.; ALMINSHID, A. H.; ALJAAFARI, H. A. S. Promising evolution of biofuel generations. Subject review. **Renewable Energy Focus**, v. 28, p. 127–139, March 1. 2019.

ANTONETTI, C. et al. Microwave-assisted dehydration of fructose and inulin to HMF catalyzed by niobium and zirconium phosphate catalysts. **Applied Catalysis B: Environmental**, v. 206, p. 364–377, June 5. 2017a.

ANTONETTI, C. et al. Amberlyst A-70: A surprisingly active catalyst for the MW-assisted dehydration of fructose and inulin to HMF in water. **Catalysis Communications**, v. 97, p. 146–150, June 5. 2017b.

ÁVILA, P. F.; FORTE, M. B. S.; GOLDBECK, R. Evaluation of the chemical composition of a mixture of sugarcane bagasse and straw after different pretreatments and their effects on commercial enzyme combinations for the production of fermentable sugars. **Biomass and Bioenergy**, v. 116, p. 180–188, September 1. 2018.

AYODELE, B. V.; ALSAFFAR, M. A.; MUSTAPA, S. I. An overview of integration opportunities for sustainable bioethanol production from first- and second-generation sugar-based feedstocks. **Journal of Cleaner Production**, v. 245, p. 118857, February 1. 2020.

BHATIA, S. K. et al. Recent developments in pretreatment technologies on lignocellulosic biomass: Effect of key parameters, technological improvements, and challenges. **Bioresource Technology**, v. 300, p. 122724, March 1. 2020.

BHAUMIK, P.; DHEPE, P. L. Solid acid catalyzed synthesis of furans from carbohydrates. **Catalysis Reviews - Science and Engineering**, v. 58, n. 1, p. 36–112, January 2. 2016.

BRODEUR, G. et al. Chemical and physicochemical pretreatment of lignocellulosic biomass: a review. **Enzyme research**, v. 2011, n. 1, 2011.

CAMPISI, S. et al. A Rational Revisiting of Niobium Oxophosphate Catalysts for Carbohydrate Biomass Reactions. **Topics in Catalysis**, v. 61, n. 18–19, p. 1939–1948, November 1. 2018.

CANILHA, L. et al. Bioconversion of sugarcane biomass into ethanol: an overview about composition, pretreatment methods, detoxification of hydrolysates, enzymatic saccharification, and ethanol fermentation. **Journal of biomedicine & biotechnology**, v. 2012, 2012.

CARNITI, P. et al. Cooperative action of Brønsted and Lewis acid sites of niobium phosphate catalysts for cellobiose conversion in water. **Applied Catalysis B: Environmental**, v. 193, p. 93–102, September 15. 2016.

CARVALHO, D. M. DE et al. Assessment of chemical transformations in eucalyptus, sugarcane bagasse and straw during hydrothermal, dilute acid, and alkaline pretreatments. **Industrial Crops and Products**, v. 73, p. 118–126, October 1. 2015.

CATRINCK, M. N. et al. One-step process to produce furfural from sugarcane bagasse over niobium-based solid acid catalysts in a water medium. **Fuel Processing Technology**, v. 207, p. 106482, October 1. 2020.

CATRINCK, M. N. et al. Phosphate Enrichment of Niobium-Based Catalytic Surfaces in Relation to Reactions of Carbohydrate Biomass Conversion: The Case Studies of Inulin Hydrolysis and Fructose Dehydration. **Catalysts**, v. 11, n. 9, p. 1077, 2021.

CHAREONLIMKUN, A. et al. Reactions of C5 and C6-sugars, cellulose, and lignocellulose under hot compressed water (HCW) in the presence of heterogeneous acid catalysts. **Fuel**, v. 89, n. 10, p. 2873–2880, October 1. 2010.

CHEAH, W. Y. et al. Pretreatment methods for lignocellulosic biofuels production: current advances, challenges and future prospects. **Biofuel Research Journal**, v. 7, n. 1, p. 1115–1127, March 1. 2020.

CHEN, Y. W.; LEE, H. V. Recent progress in homogeneous Lewis acid catalysts for the transformation of hemicellulose and cellulose into valuable chemicals, fuels, and nanocellulose. **Reviews in Chemical Engineering**, v. 36, n. 2, p. 215–235, 2020.

CHOUDHARY, V. et al. Xylose isomerization to xylulose and its dehydration to furfural in aqueous media. **ACS Catalysis**, v. 1, n. 12, p. 1724–1728, December 2. 2011.

CHOUDHARY, V.; SANDLER, S. I.; VLACHOS, D. G. Conversion of xylose to furfural using Lewis and Brønsted acid catalysts in aqueous media. **ACS Catalysis**, v. 2, n. 9, p. 2022–2028, September 7. 2012.

COMPANHIA NACIONAL DE ABASTECIMENTO. **Acompanhamento da safra brasileira - Cana de açúcar- safra 2022/23 - 1°levantamento**. [s.l: s.n.].

COSTA, S. M. et al. Use of sugar cane straw as a source of cellulose for textile fiber production. **Industrial Crops and Products**, v. 42, n. 1, p. 189–194, March 1. 2013.

DA SILVA, A. S. A. et al. Milling pretreatment of sugarcane bagasse and straw for enzymatic hydrolysis and ethanol fermentation. **Bioresource Technology**, v. 101, n. 19, p. 7402–7409, October 1. 2010.

DE ABREU, L. G. F. et al. Energy cane vs sugarcane: Watching the race in plant development. **Industrial Crops and Products**, v. 156, p. 112868, November 15. 2020.

DENG, W. et al. Catalytic conversion of lignocellulosic biomass into chemicals and fuels. **Green Energy & Environment**, July 20. 2022.

DIAS, M. O. S. et al. Integrated First and Second Generation Ethanol Production from Sugarcane. **Chemical Engineering Transactions**, v. 37, p. 445–450, June 20. 2014.

DUPONT. **Dupont**. Disponível em: <https://dws.octochemstore.com/>. Acesso em: 29 nov. 2022.

FAO. **World Food and Agriculture – Statistical Yearbook 2021**. Rome: [s.n.].

FORMANN, S. et al. **Beyond Sugar and Ethanol Production: Value Generation Opportunities Through Sugarcane Residues**. **Frontiers in Energy Research**Frontiers Media S.A., , nov. 2020.

GALBE, M.; WALLBERG, O. Pretreatment for biorefineries: a review of common methods for efficient utilisation of lignocellulosic materials. **Biotechnology for Biofuels 2019 12:1**, v. 12, n. 1, p. 1–26, 23 dez. 2019.

GNANSOUNOU, E. Production and use of lignocellulosic bioethanol in Europe: Current situation and perspectives. **Bioresource Technology**, v. 101, n. 13, p. 4842–4850, July 1. 2010.

GÓMEZ BERNAL, H.; BERNAZZANI, L.; RASPOLLI GALLETTI, A. M. Furfural from corn stover hemicelluloses. A mineral acid-free approach. **Green Chemistry**, v. 16, n. 8, p. 3734–3740, July 1. 2014.

GRASSI, M. C. B.; PEREIRA, G. A. G. Energy-cane and RenovaBio: Brazilian vectors to boost the development of Biofuels. **Industrial Crops and Products**, v. 129, p. 201–205, March

1. 2019.

GUILHERME, A. A. et al. EVALUATION OF COMPOSITION, CHARACTERIZATION AND ENZYMATIC HYDROLYSIS OF PRETREATED SUGAR CANE BAGASSE. **Brazilian Journal of Chemical Engineering**, v. 32, n. 1, p. 23–33, January 1. 2015.

HARAHAP, B. M. Degradation Techniques of Hemicellulose Fraction from Biomass Feedstock for Optimum Xylose Production: A Review. **Jurnal Keteknikan Pertanian Tropis dan Biosistem**, v. 8, n. 2, p. 107–124, 2020.

HE, L. et al. One-pot synthesis of dimethyl succinate from d-fructose using Amberlyst-70 catalyst. **Molecular Catalysis**, v. 508, p. 111584, May 1. 2021.

HOUGHTON, R. A. Biomass. **Encyclopedia of Ecology, Five-Volume Set**, p. 448–453, January 1. 2008.

HOUGHTON, R. A.; NATIONAL RENEWABLE ENERGY LABORATORY, N.; HOUGHTON, R. A. Biomass. **Encyclopedia of Ecology, Five-Volume Set**, p. 448–453, January 1. 2008.

International Energy Agency. 2019.

ISIKGOR, F. H.; BECER, C. R. Lignocellulosic biomass: a sustainable platform for the production of bio-based chemicals and polymers. **Polymer Chemistry**, v. 6, n. 25, p. 4497–4559, June 16. 2015.

JÖNSSON, L. J.; ALRIKSSON, B.; NILVEBRANT, N. O. **Bioconversion of lignocellulose: Inhibitors and detoxification**. **Biotechnology for Biofuels,**BioMed Central, 2013.

KABBOUR, M.; LUQUE, R. Furfural as a platform chemical: From production to applications. **Biomass, Biofuels, Biochemicals: Recent Advances in Development of Platform Chemicals**, p. 283–297, January 1. 2020.

KANG, S. et al. Sustainable production of fuels and chemicals from biomass over niobium based catalysts: A review. **Catalysis Today**, v. 374, p. 61–76, August 15. 2021.

KIM, T. H. et al. Pretreatment of corn stover by aqueous ammonia. **Bioresource Technology**, v. 90, n. 1, p. 39–47, October 1. 2003.

LALUCE, C. et al. Effects of pretreatment applied to sugarcane bagasse on composition and morphology of cellulosic fractions. **Biomass and Bioenergy**, v. 126, p. 231–238, July 1. 2019.

LEYVA, F. et al. Kinetics of propionic acid and isoamyl alcohol liquid esterification with amberlyst 70 as catalyst. **Industrial and Engineering Chemistry Research**, v. 52, n. 51, p. 18153–18161, December 26. 2013.

LI, H. et al. Investigation of lignin deposition on cellulose during hydrothermal pretreatment, its effect on cellulose hydrolysis, and underlying mechanisms. **Biotechnology and Bioengineering**, v. 111, n. 3, p. 485–492, March 1. 2014.

LI, X.; JIA, P.; WANG, T. Furfural: A Promising Platform Compound for Sustainable Production of C4 and C5 Chemicals. **ACS Catalysis**, v. 6, n. 11, p. 7621–7640, November 4. 2016.

LIU, X. et al. Efficient Reaction Systems for Lignocellulosic Biomass Conversion to Furan Derivatives: A Minireview. **Polymers 2022, Vol. 14, Page 3671**, v. 14, n. 17, p. 3671, September 4. 2022.

LOTT, M. C.; PYE, S.; DODDS, P. E. Quantifying the co-impacts of energy sector decarbonisation on outdoor air pollution in the United Kingdom. **Energy Policy**, v. 101, p. 42–

51, 2017.

LOU, W. Y. et al. A Highly Active Bagasse-Derived Solid Acid Catalyst with Properties Suitable for Production of Biodiesel. **ChemSusChem**, v. 5, n. 8, p. 1533–1541, August 1. 2012.

LU, S. et al. Saccharification of sugarcane bagasse by magnetic carbon-based solid acid pretreatment and enzymatic hydrolysis. **Industrial Crops and Products**, v. 160, p. 113159, February 1. 2021.

LUZ, S. M. et al. Thermal Properties of Polypropylene Composites Reinforced with Different Vegetable Fibers. **Advanced Materials Research**, v. 123–125, p. 1199–1202, 2010.

MANKAR, A. R. et al. Pretreatment of lignocellulosic biomass: A review on recent advances. **Bioresource Technology**, v. 334, p. 125235, August 1. 2021.

MARIANA NEVES CATRINCK. **The use of niobium-based solid acid catalysts in the reactions of biomass valorization**. Doctor Scientiae—Viçosa: Universidade Federal de Viçosa, 2018.

MARTINS, F. et al. Analysis of Fossil Fuel Energy Consumption and Environmental Impacts in European Countries. **Energies 2019, Vol. 12, Page 964**, v. 12, n. 6, p. 964, March 13. 2019.

MAT ARON, N. S. et al. Sustainability of the four generations of biofuels – A review. **International Journal of Energy Research**, v. 44, n. 12, p. 9266–9282, October 10. 2020.

MATSUOKA, S. et al. Energy Cane: Its Concept, Development, Characteristics, and Prospects. **Advances in Botany**, v. 2014, p. 1–13, September 30. 2014.

MORAIS DE CARVALHO, D. et al. Isolation and characterization of acetylated glucuronoarabinoxylan from sugarcane bagasse and straw. **Carbohydrate Polymers**, v. 156, p. 223–234, January 20. 2017.

NAIK, S. N. et al. **Production of first and second generation biofuels: A comprehensive review**. **Renewable and Sustainable Energy Reviews,** Pergamon, 2010.

NEGRÃO, D. R. et al. Inorganics in sugarcane bagasse and straw and their impacts for bioenergy and biorefining: A review. **Renewable and Sustainable Energy Reviews**, v. 148, p. 111268, September 1. 2021.

NICULA DE CASTRO, R. E.; BRITO ALVES, R. M.; OLLER NASCIMENTO, C. A. Assessing the sugarcane bagasse and straw as a biofuel to propel light vehicles. **Sustainable Energy & Fuels**, v. 5, n. 9, p. 2563–2577, May 4. 2021.

NIGAM, P. S.; SINGH, A. Production of liquid biofuels from renewable resources. **Progress in Energy and Combustion Science**, v. 37, n. 1, p. 52–68, February 1. 2011.

NITSOS, C. K.; MATIS, K. A.; TRIANTAFYLLIDIS, K. S. Optimization of hydrothermal pretreatment of lignocellulosic biomass in the bioethanol production process. **ChemSusChem**, v. 6, n. 1, p. 110–122, January 1. 2013.

NOVACANA. **Listas de Usinas de Açúcar e Etanol do Brasil**. Disponível em: <https://www.novacana.com/usinas_brasil/estados>. Acesso em: 11 nov. 2022.

OUR WORLD IN DATA. **Energy mix**. Disponível em: <https://ourworldindata.org/energy-mix>. Acesso em: October 11. 2022.

OYEDEJI, O. et al. Understanding the Impact of Lignocellulosic Biomass Variability on the Size Reduction Process: A Review. **ACS Sustainable Chemistry and Engineering**, v. 8, n. 6, p. 2327–2343, February 11. 2020.

PALMA, K. R. DE et al. The influence of the elemental and structural chemical composition on the ash fusibility of sugarcane bagasse and sugarcane straw. **Fuel**, v. 304, November 15. 2021.

PAPAKONSTANTINOU, E. et al. Materials of biological origin and biofuels: Small environmental footprint and epigenetic impact (Review). **International Journal of Epigenetics**, v. 1, n. 3, p. 1–8, September 1. 2021.

PEREA-MORENO, M. A.; SAMERÓN-MANZANO, E.; PEREA-MORENO, A. J. Biomass as Renewable Energy: Worldwide Research Trends. **Sustainability 2019, Vol. 11, Page 863**, v. 11, n. 3, p. 863, February 7. 2019.

PROBST, K. V. et al. The effect of moisture content on the grinding performance of corn and corncobs by hammermilling. **Transactions of the ASABE**, v. 56, n. 3, p. 1025–1033, 2013.

RENTIZELAS, A. A. Biomass storage. **Biomass Supply Chains for Bioenergy and Biorefining**, p. 127–146, January 1. 2016.

ROCHA, G. J. DE M. et al. Influence of mixed sugarcane bagasse samples evaluated by elemental and physical–chemical composition. **Industrial Crops and Products**, v. 64, p. 52–58, 1 February. 2015.

RUIZ, H. A.; THOMSEN, M. H.; TRAJANO, H. L. Hydrothermal Processing in Biorefineries: Production of Bioethanol and High Added-Value Compounds of Second and Third Generation Biomass. **Hydrothermal Processing in Biorefineries: Production of Bioethanol and High Added-Value Compounds of Second and Third Generation Biomass**, p. 1–511, June 1. 2017.

SAAD, M. B. W. et al. Preliminary studies on fungal treatment of sugarcane straw for organosolv pulping. **Enzyme and Microbial Technology**, v. 43, n. 2, p. 220–225, August 5. 2008.

SEGAL, L. et al. An Empirical Method for Estimating the Degree of Crystallinity of Native Cellulose Using the X-Ray Diffractometer. **http://dx.doi.org/10.1177/004051755902901003**, v. 29, n. 10, p. 786–794, July 2. 2016.

SIRIL, P. F.; CROSS, H. E.; BROWN, D. R. New polystyrene sulfonic acid resin catalysts with enhanced acidic and catalytic properties. **Journal of Molecular Catalysis A: Chemical**, v. 279, n. 1, p. 63–68, January 2. 2008.

SLUITER, A. et al. Determination of Structural Carbohydrates and Lignin in Biomass: Laboratory Analytical Procedure (LAP) (Revised July 2011). 2008.

SOLTANIAN, S. et al. A critical review of the effects of pretreatment methods on the exergetic aspects of lignocellulosic biofuels. **Energy Conversion and Management**, v. 212, p. 112792, May 15. 2020.

SUDARSANAM, P.; LI, H.; SAGAR, T. V. TiO2-Based Water-Tolerant Acid Catalysis for Biomass-Based Fuels and Chemicals. **ACS Catalysis**, v. 10, n. 16, p. 9555–9584, August 20. 2020.

SZCZERBOWSKI, D. et al. Sugarcane biomass for biorefineries: Comparative composition of carbohydrate and non-carbohydrate components of bagasse and straw. **Carbohydrate Polymers**, v. 114, p. 95–101, December 19. 2014.

TURSI, A. A review on biomass: importance, chemistry, classification, and conversion. **Biofuel Research Journal**, v. 6, n. 2, p. 962–979, June 1. 2019.

VIEIRA, J. L. et al. Niobium phosphates as bifunctional catalysts for the conversion of biomass-

derived monosaccharides. **Applied Catalysis A: General**, v. 617, p. 118099, May 5. 2021.

VILCOCQ, L. et al. Hydrolysis of Oligosaccharides Over Solid Acid Catalysts: A Review. **ChemSusChem**, v. 7, n. 4, p. 1010–1019, April 1. 2014.

WANG, T. et al. A review of the hydrothermal carbonization of biomass waste for hydrochar formation: Process conditions, fundamentals, and physicochemical properties. **Renewable and Sustainable Energy Reviews**, v. 90, p. 223–247, July 1. 2018.

YOSHIDA, K. et al. Furfural production from xylose and bamboo powder over chabazite-type zeolite prepared by interzeolite conversion method. **Journal of the Taiwan Institute of Chemical Engineers**, v. 79, p. 55–59, October 1. 2017.

YU, I. K. M. et al. Chemicals from lignocellulosic biomass: A critical comparison between biochemical, microwave and thermochemical conversion methods. **https://doi.org/10.1080/10643389.2020.1753632**, v. 51, n. 14, p. 1479–1532, 2020.

ZHU, J.; HUANG, Y. Solid-state NMR study of dehydration of layered α-niobium phosphate. **Inorganic Chemistry**, v. 48, n. 21, p. 10186–10192, November 2. 2009.

ZIOLKOWSKA, J. R. Biofuels technologies: An overview of feedstocks, processes, and technologies. **Biofuels for a More Sustainable Future: Life Cycle Sustainability Assessment and Multi-Criteria Decision Making**, p. 1–19, January 1. 2020.

ZOGHLAMI, A.; PAËS, G. Lignocellulosic Biomass: Understanding Recalcitrance and Predicting Hydrolysis. December 18. 2019, p. 874.